energy&fuels

pubs.acs.org/EF Article

Petroleomics Approach to Investigate the Composition of Upgrading Products from Pyrolysis Bio-Oils as Determined by High-Field FT-ICR MS

Published as part of the Energy & Fuels virtual special issue "Highlighting Contributions from Our Editorial Board Members (2023)".

Martha L. Chacón-Patiño, Charlotte Mase, Julien Florent Maillard, Caroline Barrère-Mangote, David C. Dayton, Carlos Afonso, Pierre Giusti, and Ryan P. Rodgers*

Cite This: https://doi.org/10.1021/acs.energyfuels.3c02599 Read Online

ACCESS | Metrics & More | Article Recommendations | Supporting Information

ABSTRACT: One of the few similarities between petroleum and bio-oils derived from biomass pyrolysis is that they are both complex organic mixtures composed of thousands of distinct elemental compositions, but biomass pyrolysis oils uniquely contain ultrahigh oxygen content and a more diverse collection of chemical functionalities. Thus, their chemistry is different from fossil fuels, and advanced upgrading strategies for the coprocessing of such unique materials along with conventional refinery feeds will benefit from comprehensive knowledge of their molecular composition, known as petroleomics. The work presented herein focuses on the molecular characterization of nonvolatile species from a loblolly pine bio-oil and its hydrotreated effluents by soft ionization methods coupled to high-field Fourier transform ion cyclotron resonance mass spectrometry (FT-ICR MS). Electrospray ionization (ESI) facilitates the analysis of polar oxygen-containing molecules, whereas atmospheric pressure chemical ionization (APCI) enables access to hydrocarbons. The molecular data revealed time-dependent compositional changes, visualized in van Krevelen diagrams, that highlighted the optimal catalyst performance and the impacts of catalyst fouling or deactivation. Furthermore, elucidation of compositional features such as abundance-weighted H/C, O/C, molecular weight, and aromaticity facilitated data interpretation and suggested that value-added bio-oils are likely produced upon a concurrent decrease in oxygen content, aromaticity, and molecular weight with a marked increase in H/C. Furthermore, distinct temporal molecular changes suggested specific hydrotreatment reaction pathways, including concurrent deoxygenation and hydrogenation, transalkylation, and cracking of highly aromatic lignin-like oligomers. The detailed molecular characterization provided by FT-ICR MS facilitated access to common molecular formulas (those detected both before and after upgrading). Common formulas are hypothetically recalcitrant compounds, which feature a highly aromatic nature (low H/C) and alkyl deficiency. Understanding the chemistry of such molecules, along with the remaining oxygen-containing species, is critical for future advances in bio-oil upgrading.

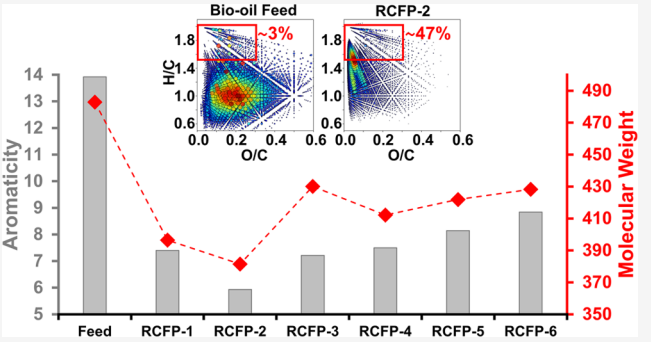

INTRODUCTION

Alternative fuels from biomass fast pyrolysis are promising "green" energy sources with the potential to offset carbon emissions.[1] Indeed, fast pyrolysis of biomass has been the target of extensive scientific efforts since the oil crisis in the mid-1970s, with significant advances in catalyst development for hydrotreatment achieved in the past decade.[2−5] Thus, current biomass pyrolysis methods can produce liquid intermediates that can be upgraded to obtain hydrocarbon molecules with properties consistent with transportation fuels.[6−10]

The generation of renewable fuels from biomass involves the critical steps of feedstock purification, thermal deconstruction of biomass polymers, chemical modification such as heteroatom removal and cracking, and separations to implement molecular management.[11] Initially, pyrolysis transforms biomass into condensable volatiles or bio-oil, noncondensable gases, and biochar, which occurs through the decomposition of

Received: July 14, 2023
Revised: September 18, 2023

polymer chains of cellulose, hemicellulose, and lignin.[12−18] As a result, bio-oils are ultracomplex mixtures with a wide range of oxygen content, chemical functionalities, molecular weight, and thermal stability. Indeed, the chemistries of bio-oils and fossil fuels are very dissimilar.[19,20] For instance, bio-oils feature much higher oxygen concentration and acidity, which translates into poor thermal stability and prevents their processing through well-established petroleum-refining methods.[21−23] A typical vacuum gas oil from heavy petroleum features an oxygen content of <1 wt %, H/C of ∼1.6, density <1 g/mL, neutral pH, and boiling points between 160 and 400 °C.[15,24] In contrast, typical pyrolysis bio-oils reveal oxygen contents up to ∼40 wt %, H/C of ∼1.3, densities between ∼1.10 and 1.30 g/mL, acidic pH between 2 and 3, and undefined boiling range as they decompose upon heating.[25−27]

Loblolly pine is a preferred wood source for fast pyrolysis of biomass, with an average content of lignin, cellulose, and hemicellulose of ∼31, ∼37, and ∼23%, respectively.[28−36] Loblolly pine sawdust has been successfully transformed into bio-oil by reactive catalytic fast pyrolysis (RCFP), a process in which reactive gases, such as hydrogen, are incorporated to promote selective hydrodeoxygenation and decrease char yields.[37] Several works have shown that RCFP with molybdenum oxide-based catalysts can produce higher bio-oil yields with improved chemistry, e.g., much lower oxygen contents and higher H/C ratios.[37−39] Many of these efforts have investigated catalyst selection and the effect of H_2 pressure.[37,40] Recently, Cross et al.[38] concluded that an optimal H_2 partial pressure significantly drives the transformation of phenols and carbonyls, which yields bio-oils with lower O/C ratios. Specifically, RCFP promotes the deoxygenation of anhydrosugars and poly-methoxy phenols, which enables the production of bio-oils that could be further upgraded into transportation fuels.[37,41]

Bio-oil upgrading seeks the generation of high carbon yields with high H/C and substantially decreased O/C ratios.[42,43] Generally, catalytic hydrodeoxygenation (HDO) at a temperature of ∼400 °C and a H_2 pressure of ∼135 bar can induce significant deoxygenation; some reports have suggested up to ∼99.5% of oxygen removal.[26,44−49] However, oxygen-depleted, upgraded bio-oils still feature significant molecular-level differences from fossil fuels. For instance, distillation cuts from the North Slope crude have revealed superior concentrations of paraffins (up to ∼8-fold higher) and increased H/C ratios (*e.g.*, H/C = 1.75 vs 1.55) than upgraded bio-oils with minimal amounts of oxygen.[11,50,51] Therefore, removing recalcitrant oxygen is not the only goal of bio-oil upgrading; producing molecules that resemble those of petroleum-derived fuels is also necessary.

Recent advances in HDO processes under low hydrogen partial pressure have shown promising results for oxygen removal and hydrogenation of model compounds such as phenols, ketones, and furans.[52,53] Several works suggest that *ex situ* HDO assisted by molybdenum-based catalysts (*e.g.*, MoO_3) can increase the production of hydrocarbons, with yields close to ∼30 C% and high concentration of aromatics (∼7 C%) and alkanes (∼18 C%).[54,55] These advances emphasize the transformation of low-molecular-weight O-containing compounds into species with a higher content of alkyl moieties and lower oxygen concentrations. However, abundant compounds remain enriched with carboxylic acids and anhydrosugars. It is essential to highlight that carbonyl compounds are challenging to remove, and only moderate transformation efficiencies under high pressures and temperatures have been reported.[56]

Understanding bio-oil molecular composition is central to improving bio-oil production and refinery, which can rely on the lessons learned from petroleum analysis by mass spectrometry (MS). The use of ultra-high-resolution MS to investigate the ultracomplex composition of fossil fuels, complemented by bulk techniques such as combustion elemental analysis and NMR spectroscopy, is known as *petroleomics*.[57−60] Its ultimate goal is to predict petroleum behavior and improve upstream and downstream operations based on molecular-level knowledge.[61,62] Petroleomics relies on the ultrahigh resolving power and mass accuracy uniquely provided by high-field Fourier transform ion cyclotron resonance mass spectrometry (FT-ICR MS). This technique can access tens of thousands of molecules present in complex mixtures. Over the last two decades, it has enabled an in-depth understanding of the wide diversity of molecules in heavy petroleum and proved its continuum composition, a concept originally proposed by Boduszynski in the early 1980s.[63,64] This knowledge provided the petroleum community with the tools to predict distillation trends, understand and solve deposit formation in production facilities, and design better strategies for petroleum refining. Furthermore, the implementation of separation methods, such as extrography and column chromatography coupled to FT-ICR MS, also provided knowledge of the structures in heavy feedstocks and asphaltenes.[65,66] One of the major lessons learned is that separation strategies are crucial to achieving comprehensive characterization by FT-ICR MS and that the higher the heteroatom content, the more difficult it is to develop and implement such separations.

The development of efficient upgrading technologies for renewable fuels requires a comprehensive understanding of bio-oil molecular composition.[67,68] Two-dimensional gas chromatography, GC × GC, has dominated the field of chemical analysis for the volatile fraction of bio-oils and has been notably helpful to semiquantitatively classify compound families such as alkanes, cycloalkanes, and aromatics.[69−71] However, the nonvolatile fraction requires advanced instrumentation, such as high-field FT-ICR MS, as a large mass fraction of pyrolysis bio-oils are ultracomplex, nondistillable mixtures of polyfunctional O-containing molecules.[72,73] A typical bio-oil analysis by FT-ICR MS produces tens of thousands of mass spectral peaks. Ideally, each peak is assigned a unique molecular formula based on mass accuracy and isotopic patterns.[74,75] In general, molecular formulas are sorted into heteroatom classes; for instance, the O_3 class comprises all of the species with C, H, and three oxygen atoms. Common data representations include plots of double bond equivalents (DBE = number of rings plus double bonds to carbon) versus carbon number and van Krevelen diagrams of atomic ratios such as H/C versus O/C.[76]

Several research groups have used electrospray ionization (ESI) and atmospheric pressure photoionization (APPI) for targeted analysis of polar and aromatic bio-oil species.[59,77,78] For instance, Jarvis et al.[77] reported the −ESI FT-ICR MS investigation of bio-oils derived from different biomass sources such as oak, mixed conifer, and scotch broom. The authors found molecules composed mainly of C, H, and up to 13 oxygen atoms (O_{13} class). This study highlighted the identification of boron-containing compounds ($^{11}BO_X$, X = 4−12), which can be readily misassigned as N_2O_X species due

https://doi.org/10.1021/acs.energyfuels.3c02599
Energy Fuels XXXX, XXX, XXX−XXX

to a mass difference of only 35 μDa, which highlights the need for ultrahigh mass resolving power, only achievable by FT-ICR MS.[77] In other reports, Ware et al.[79,80] performed a detailed analysis of oak bio-oils and their hydrotreated products via +APPI FT-ICR MS. The accessed compositional range featured DBE values from ∼5 to ∼25, carbon numbers between 8 and 46, H/C ratios of 0.5−1.5, and up to 14 oxygen atoms per molecule. The authors noted that bio-oil composition revealed a concurrent monotonic increase in DBE and carbon number as a function of increasing the number of oxygen atoms, which suggested the presence of oligomeric species. In contrast, the hydrotreated products featured a compositional range that narrowed in the DBE and carbon number as a function of increasing oxygen content, which suggested the occurrence of direct deoxygenation. Indeed, compound classes with high oxygen numbers (>7) maintained their initial DBE upon hydrotreating, which ruled out hydrogenation reaction pathways.[79] In another study, Palacio Lozano et al.[81] used van Krevelen diagrams for data mining of −ESI FT-ICR MS analysis of bio-oils. The authors suggested reaction pathways, such as dehydration and decarboxylation, based on specific changes in H/C and O/C ratios upon bio-oil upgrading. Furthermore, the authors proposed categorizing bio-oil molecules in three zones according to their location in van Krevelen diagrams. In such classification, compounds with high energy density and elemental compositions similar to fossil fuels feature $1.5 \leq H/C < 2$, $0 < O/C \leq 0.3$, and belong to *zone 1*. Conversely, molecules with little to no potential of being used as fuels are in *zone 2* and present extremely low H/C ratios and a wide range of oxygen content ($0.5 < H/C < 1.5$, $0 < O/C < 0.67$). Finally, species that can be easily transformed into molecules with high energy density, throughout deoxygenation pathways, are contained in *zone 3* and present $1.5 < H/C < 2$, $O/C > 0.3$.[81]

ESI and APPI ion sources are helpful to access polar and aromatic compounds. However, bio-oil upgrading can produce significant amounts of (nonpolar) hydrocarbons that could be difficult to ionize by those ionization methods due to selective ionization. Recently, Mase et al.[82] used atmospheric pressure chemical ionization (APCI) to target the analysis of hydrocarbons and aromatic species in pine bio-oils. The authors compared the compositional range accessed via different ion sources, *i.e.*, APPI, ESI, and APCI, with different ionization "additives" such as formic acid or sodium acetate for +ESI and methanol or *n*-heptane for APCI. Specifically, APPI allowed for the abundant ionization of molecules with high DBE, limited alkyl-chain substitution, and low oxygen content compared with ESI, which, in contrast, efficiently exposed highly polar species with increased O/C ratios. On the other hand, heptane-assisted APCI was remarkably useful to access abundant, nonpolar low-DBE compounds. One hypothesis is that the ionization of hydrocarbons can be achieved via proton-transfer reactions, which is facilitated by the use of heptane during ionization. Another theory is that ionization of hydrocarbons occurs via exothermic proton-transfer reactions involving highly acidic and protonated atmospheric molecules such as N_2 and H_2O.[83] As hydrocarbons are the desired products from upgrading, the characterization of such compounds is critical to improving the production of value-added fuels from bio-oils.

The work herein is the first of a series of manuscripts dealing with the application of petroleomics principles to comprehend the molecular composition of bio-oils. In this work, the molecular characterization of a loblolly pine bio-oil and its hydrotreated effluents was performed by +APCI and −ESI coupled to 12 and 21 T FT-ICR MS. These analyses exposed complementary compositional trends for hydrocarbons and highly oxygenated molecules that could help determine optimal hydrotreating conditions and understand reaction pathways.

MATERIALS AND METHODS

Bio-Oil Production and Upgrading. Samples were supplied by RTI International, North Carolina. Bio-oil was produced from the reactive catalytic fast pyrolysis (RCFP) of loblolly pine. The RCFP was performed under 80 vol % hydrogen in a laboratory-scale pyrolysis reactor (2.5 inch diameter fluidized bed reactor) with a molybdenum catalyst, at an average temperature of 500 °C and biomass feed rate of about 4−5 g per minute. Bio-oil, obtained from RCFP of loblolly pine, was hydrotreated continuously for 144 h under 2000 psi of H_2. In total, 9.0 kg of bio-oil was fed into a pilot-scale hydroprocessing unit.[4] Specifically, the RCFP biocrude (referred to as bio-oil feed) was hydrotreated continuously for 144 h in an RTI's pilot-scale hydroprocessing unit at 2000 psi of hydrogen pressure and a liquid hourly space velocity (LHSV) of 0.35/h over a sulfide hydrotreating catalyst. The average reactor bed temperature was 300 °C. A total of 9.0 kg of feed was processed. Information about the catalyst is reported elsewhere.[4] Six effluents were recovered at different time points: ∼36.5, 48.5, 72.5, 96.5, 124.5, and 143.5 h. Thus, the hydrotreated effluents could be used to access catalyst aging and were labeled RCFP-1−6. Much more detail on the production and upgrading of the RCFP biocrude can be found in the literature.[4]

Reagents. High-performance liquid chromatography (HPLC)-grade methanol and toluene were purchased from J.T. Baker Chemicals, Phillipsburg, NJ. Tetramethylammonium hydroxide (TMAH 25 vol % in methanol) was obtained from Fisher Scientific. Toluene and *n*-heptane solvents, with a purity higher than 99.7%, were purchased from VWR chemicals and used for APCI 12 T FT-ICR MS.

Elemental Analyses. Bio-oil and its hydrotreated effluents were subjected to bulk elemental analysis for C, H, and S, conducted with a Thermo FLASH 2000 analyzer (Thermo Fisher Scientific, MA). In addition, the oxygen content was accessed using a Flash SMART analyzer from Thermo Fisher Scientific. Oxygen measurements require correction of the contribution from water by measuring its content in wt % using the traditional Karl Fisher technique. The molecular weight of water is 18.015 Da, in which oxygen accounts for 15.999 Da (88.8%). Both water and oxygen contents are measured in wt %; thus, 88.8% of the water content is subtracted from the measured oxygen content by elemental analysis in order to obtain water-free oxygen. Nitrogen was measured with a Mitsubishi TN2100 V analyzer equipped with a vertical oven VF-210, an ND-210 chemiluminescence detector, and a thermostatic passer STC-210L.

Ultra-High-Resolution Mass Spectrometry. *Positive-Ion APCI Coupled to 12 T FT-ICR MS.* For direct infusion APCI experiments, bio-oils and the upgraded effluents were first solubilized at 10 mg/mL in a 1/1 (v/v) toluene/methanol mixture. Samples were diluted at 0.5 mg/mL in *n*-heptane to promote ionization of alkanes in APCI.[84] Heptane was used to avoid the mass spectral chemical noise commonly encountered with isooctane. Analyses were performed on an FT-ICR MS instrument equipped with a 12 T superconducting magnet and a dynamically harmonized ICR cell (SolariX 2XR, Bruker Daltonics, Bremen, Germany). The mass spectrometer was externally calibrated with a solution of sodium trifluoroacetate. Sample solutions were directly infused into the APCI source at a flow rate of 600 μL/h. Mass spectra were acquired in positive-ion mode over m/z 92−1000, at 4 million data points with 1.05 s transient length and coaddition of 200 scans, which yielded a resolution of 552,000 at m/z 200. Ionization and ion transferring were carried out at a capillary voltage of 4000 V, end plate offset of −500 V, corona needle at 4000 nA, nebulizer gas of 1 bar, vaporizer temperature of 350 °C, dry gas flow

https://doi.org/10.1021/acs.energyfuels.3c02599
Energy Fuels XXXX, XXX, XXX−XXX

Table 1. Bulk Elemental Composition for the Bio-Oil Feed and the Hydrotreated Effluents

sample	% C	% H	% N*	% S	% O*	H/C	O/C	% water content
feed	72.40	6.70	0.09	<0.50	8.30	1.11	0.09	6.91
RCFP-1	86.00	11.00	0.02	<0.50	1.01	1.53	0.01	0.05
RCFP-2	84.40	10.50	0.04	<0.50	1.65	1.49	0.01	0.13
RCFP-3	84.40	10.00	0.06	<0.50	2.71	1.42	0.02	0.38
RCFP-4	84.20	9.62	0.07	<0.50	3.50	1.37	0.03	0.57
RCFP-5	83.70	9.37	0.08	<0.50	3.96	1.34	0.04	0.85
RCFP-6	83.70	9.28	0.08	<0.50	4.29	1.33	0.04	0.97

% In weight, *N was measured using a Mitsubishi TN2100 V analyzer equipped with an ND-210 chemiluminescence detector, **water corrected.

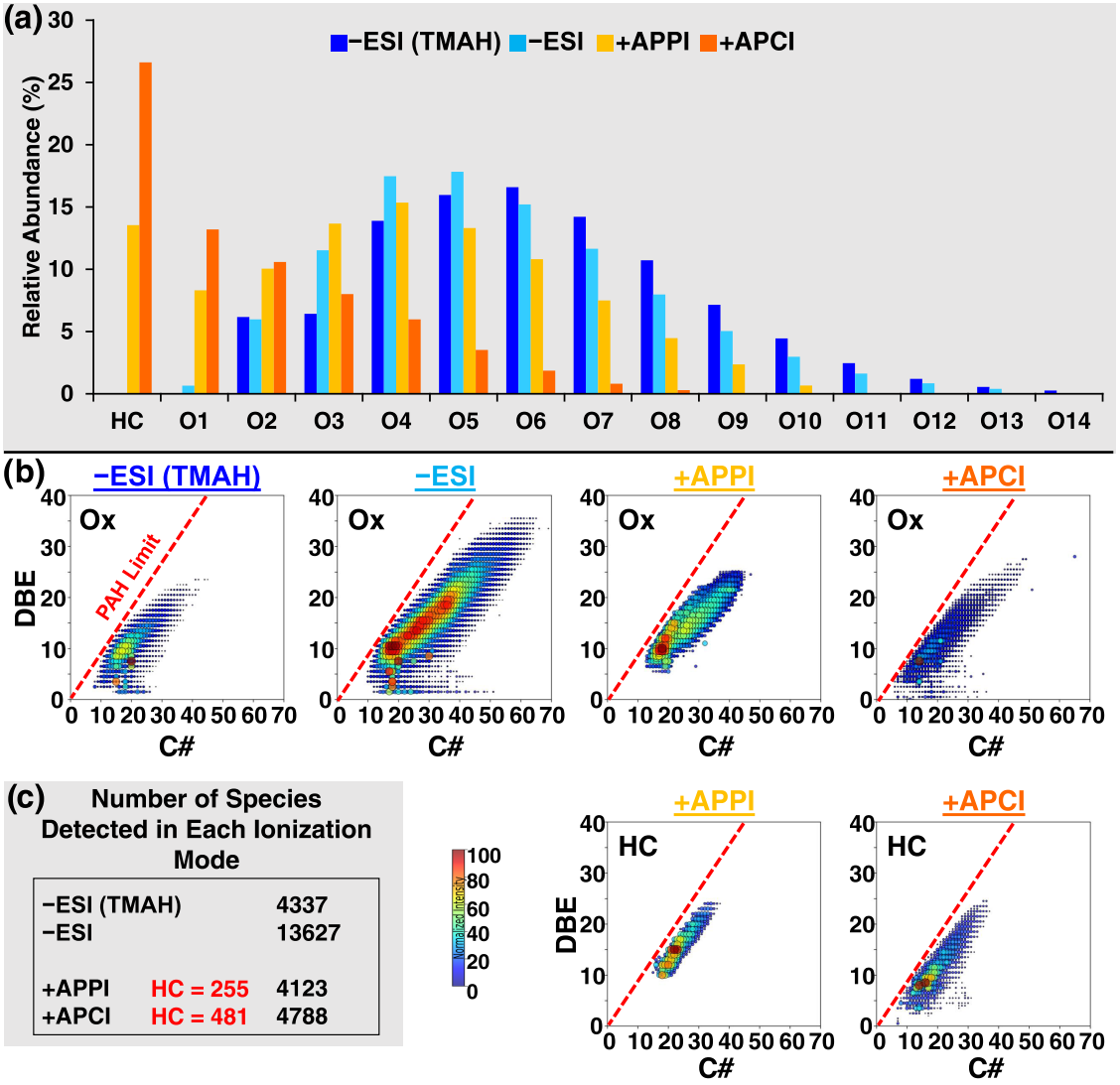

Figure 1. (a) Heteroatom class distribution derived from FT-ICR MS analysis of pyrolysis oil derived from loblolly pine (bio-oil feed), ionized by different methods: −ESI with and without deprotonation additive and +APPI were collected by 21 T FT-ICR MS, and +APCI used 12 T FT-ICR MS. (b) Combined DBE vs carbon number plots for all oxygen-containing compound classes (all ionization methods) and hydrocarbons (only positive-ion APPI and APCI). (c) Number of assigned molecular formulas for each ionization method.

of 2 L/min, dry temperature at 250 °C, and time-of-flight of 0.8 ms. Data treatment was performed with DataAnalysis Software (version 6.0, Bruker, Bremen, Germany). Each mass spectrum was internally calibrated using homologous series present over the whole mass range, which resulted in an error standard deviation of <0.3 ppm. m/z values were picked with a signal-to-noise ratio (S/N threshold) greater than 6, with both odd and even electron configurations. Molecular formulas were attributed with a maximum error of 0.5 ppm. Elemental boundaries were limited to $C_xH_yN_2O_{18}$ with maximum DBE and H/C set to 40 and 2.5.

Negative-Ion ESI and Positive-Ion APPI Coupled to 21 T FT-ICR MS. For negative-ion micro-ESI, extensively used for the characterization of oxygen-rich samples,[85] the bio-oil feed (or RCFP biocrude) and hydrotreated effluents were dissolved in 1:1 toluene/methanol at a concentration of 50 μg/mL. Samples were directly infused at 0.5 μL/min and ionized with a needle voltage of 3.2 kV. Analyses were also performed adding tetramethylammonium hydroxide (TMAH, 0.005% v/v) to the sample solutions to promote deprotonation.[86] For

https://doi.org/10.1021/acs.energyfuels.3c02599
Energy Fuels XXXX, XXX, XXX−XXX

+APPI, samples were diluted in toluene/methanol (1/1 v/v) to a concentration of 25 μg/mL and directly infused at 50 μL/min into an APPI Ion Max source (Thermo Fisher Scientific, Inc., San Jose, CA), operated with a vaporizer temperature of 300 °C. For APPI, N_2 sheath gas was used at 50 psi, N_2 auxiliary gas (32 mL/min) prevented oxidation, and gas-phase neutrals were photoionized by a 10.2 eV ultraviolet krypton lamp (Syagen Technology, Inc., Tustin, CA). Ions were analyzed with a custom-built 21 T FT-ICR mass spectrometer.[87,88] For this purpose, 1×10^6 charges were accumulated for 1−5 ms in an external multipole ion trap, equipped with automatic gain control (AGC).[88,89] Ions were subsequently transferred to the ICR cell, as a function of m/z, by a decreasing auxiliary radio frequency.[88,89] Ions were excited to an m/z-dependent radius to maximize the dynamic range and the number of detected peaks. Excitation and detection were performed on the same pair of electrodes of the dynamically harmonized ICR, operated with 6 V trapping potential. Time-domain transients of 3.2 s were acquired with Predator Software, and 100 time-domain transients were averaged for all of the samples. Mass spectra were phase-corrected and internally calibrated with oxygen-containing homologous series using the "walking" calibration method.[90] PetroOrg software assisted molecular formula calculation.[91] CSV files from all assigned molecular formulas were exported from PetroOrg and also from Data Analysis (APCI 12 T FT-ICR MS) and imported into PyC2MC for data visualization in plots of DBE vs carbon number and van Krevelen diagrams.[92] Molecular formulas with an error >0.20 ppm were discarded, and only compound classes with a relative abundance of ≥0.15% were considered. Raw mass spectra, calibrated peak lists, PetroOrg files, and lists of molecular formula assignments are publicly available at Open Science Framework, DOI 10.17605/OSF.IO/BVM65.

RESULTS AND DISCUSSION

Bulk Elemental Analysis. The hydrotreated effluents from the bio-oil feed were collected at different time points; thus, their composition could be correlated to catalyst deactivation. In a previous report, catalyst deactivation was correlated to density and H and O contents of the hydrotreated bio-oils as a function of time on stream. Specifically, the density increased as a function of increasing catalyst deactivation. However, the catalyst was active even after 144 h. of time on stream.[4] Table 1 presents the bulk elemental composition of the bio-oil feed (RCFP biocrude) and its hydrotreated effluents (RCFP-1−6). The results highlight the prominent decrease in oxygen content (up to ∼8-fold) and increase in H/C (*e.g.*, from ∼1.10 to 1.50) upon hydrotreatment; RCFP-1 (collected at 36.5 h) and RCFP-2 (48.5 h) featured the best bulk properties. Notably, the results point out a sharp rise in oxygen content from RCFP-3 (collected at 72.5 h), which suggest a loss in hydrotreatment performance likely due to catalyst deactivation. Table 1 also indicates that the S content was minimal and remained. Results from bulk elemental analysis are revisited later to understand the extent of selective ionization in mass spectral analyses.

Selection of Optimal Ionization Methods for MS Analysis. Bio-oils are ultracomplex mixtures in which MS analysis is likely limited by selective ionization, similar to what has been observed in the molecular-level characterization of fossil fuels by high-resolution mass spectrometry. As proved for petroleum, separations and the use of different ion sources operated under distinct conditions help in achieving comprehensive molecular-level analysis. Separations are the subject of future work; the focus here is comprehensive untargeted bio-oil MS characterization, which requires complementary ion sources that enable access to thousands of compounds with no significant ionization bias. Figure 1 presents the molecular composition of the feed bio-oil as determined by 12 and 21 T FT-ICR MS, assisted by +APPI and +APCI and −ESI with [tetramethylammonium hydroxide (TMAH)] and without deprotonation additive.[86]

FT-ICR MS of pyrolysis oils reveals thousands of peaks that are assigned a unique molecular formula based on mass accuracy and isotopic structure.[64,93] The assigned compositions are grouped into compound classes. For example, species with C and H, but no heteroatoms, make up the HC class, whereas formulas with C, H, and 10 oxygen atoms comprise the O_{10} class. Figure 1a presents the compound class distribution for the bio-oil feed obtained by the four ionization strategies. The results strongly suggest that −ESI with (dark-blue bars) and without (light-blue bars) deprotonation additives ionized oxygen-containing species with a highly similar class distribution. The oxygen content of most of the detected compounds ranged between that of O_2 and O_{13}. Conversely, positive-ion APPI and APCI (yellow and orange bars) favored the observation of hydrocarbons (HC class), with up to ∼27% of relative abundance observed via APCI. It is essential to point out that APPI and APCI ionized polar compounds with lower oxygen numbers than ESI. However, APPI favored the observation of ions with higher polarizability, such as O_{4-6}, compared with APCI, which revealed higher abundances for the O_{1-3} classes.

The heteroatom class distributions obtained by −ESI, with and without a deprotonation additive, are highly similar. However, panels (b) and (c) in Figure 1 reveal pronounced differences in molecular composition. Clearly, the use of TMAH favored the detection of low-DBE (<20), low-carbon-number (<40) compounds. Conversely, the lack of deprotonation additive enabled the observation of a compositional range with DBE values up to ∼35 and carbon numbers up to ∼60. Lessons learned from two decades of research in petroleomics demonstrated ionization bias toward low-molecular-weight acidic species, via −ESI with TMAH or NH_4OH, for fractions of naphthenic acids isolated from fossil fuels. Several works have suggested that separations help to overcome this limitation.[94−97] Importantly, the DBE vs carbon number plots highlight the PAH limit (red-dashed line), a compositional boundary for planar molecules with the highest possible DBE.[98−100] In the case of bio-oils, molecular formulas close to the PAH limit could correspond to structures similar to oxy-PAHs.[101] Thus, the data suggest that the studied pyrolysis oil is enriched in highly aromatic O-containing compounds.

It should be noted that ESI without deprotonation additive produced ∼3-fold lower number of ions (lower ion current), and thus, accumulation of the target number of charges (1×10^6) for FT-ICR MS required ∼3-fold longer "ion times" as measured by automatic gain control.[88,89] Regardless of this limitation, the number of detected compositions without the use of a deprotonation additive was superior. Figure 1c shows that the number of assigned molecular formulas without TMAH was ∼3-fold higher. Therefore, the rest of the discussion focuses on ionization by negative-ion ESI without TMAH as an additive.

Ionization of Hydrocarbons. +APPI and +APCI revealed subtle differences in the compositional range of the O-containing compounds (Figure 1b, upper row). However, the primary advantage of APCI is that it improved access to hydrocarbons, which is consistent with what has been learned in petroleomics; APCI revealed almost twice the number of

https://doi.org/10.1021/acs.energyfuels.3c02599
Energy Fuels XXXX, XXX, XXX−XXX

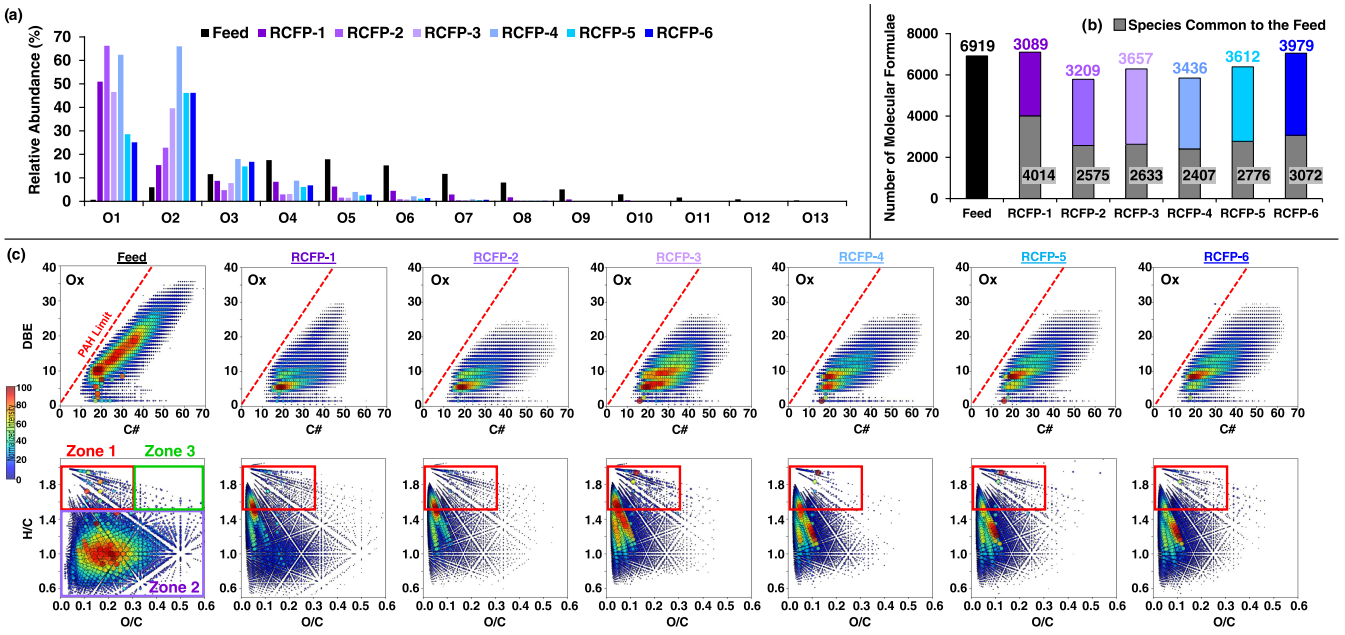

Figure 2. Molecular composition of the bio-oil feed and hydrotreated effluents (RCFP-1−6) obtained via −ESI 21 T FT-ICR MS. (a) Compound class distribution for all oxygen-containing species. (b) Number of molecular formulas detected for each sample; common formulas relative to the feed are represented in gray, whereas unique formulas to each sample are highlighted in purple/blue. (c) Combined DBE vs carbon number plots (upper row) and combined van Krevelen diagrams (lower row) for all O-containing compounds.

hydrocarbon molecular formulas than APPI (highlighted in red, Figure 1c). The accessed compositional range for hydrocarbons via APCI is much more extended, comprising DBE ∼3−25 and carbon numbers between ∼8 and 40 (Figure 1b, lower row). It is critical to highlight that using small alkanes in APCI, such as *n*-heptane (C_7), promotes the ionization of hydrocarbon species (no heteroatoms), whether saturated, unsaturated, linear, branched, or cyclic. APCI carried out with heptane enables the detection of hydrocarbons in complex mixtures. Ionization of saturated hydrocarbons occurs via exothermic proton-transfer reactions between highly acidic, protonated atmospheric molecules, such as N_2 and H_2O.[83]

Figure 2 presents the molecular composition of the bio-oil feed and hydrotreated effluents accessed via −ESI 21 T FT-ICR MS. Figure 2a shows the class distributions for all detected O-containing species. The feed revealed abundant compounds with high oxygen numbers, with up to 13 oxygen atoms and dominance of O_{4-7} classes. Conversely, the hydrotreated effluents featured higher abundances of low-order oxygen-containing classes, such as O_1 and O_2. These compositional trends suggest a high degree of deoxygenation. Notably, the effluent RCFP-2 exhibited the most promising properties for energy applications. It revealed the lowest oxygen content per molecule, as >90% of the detected species, as measured in relative abundance, had only 1−2 oxygen atoms. In contrast, the bio-oil feed revealed >80% of compounds with ≥4 oxygen atoms.

Figure 2b presents the number of assigned monoisotopic molecular formulas, unique to each sample (purple/blue) and common to the bio-oil feed (gray). Specifically, the bio-oil feed (black bar) revealed 6919 monoisotopic compositions. It is noteworthy that the high resolving power and dynamic range, facilitated by the high magnetic field of the 21 T FT-ICR mass spectrometer, enable the detection and subsequent formula assignment of higher numbers of peaks. In total, counting ^{13}C and $^{13}C_2$ isotopologues, the bio-oil feed presented 13,627 assigned molecular formulas. However, the work presented herein focuses on monoisotopic species. The results indicate that hydrotreatment did not significantly decrease the number of assigned compositions. For instance, RCFP-1 and RCFP-6 revealed similar numbers of molecular formulas to those detected in the feed. RCFP-2 featured the lowest number, 5784, which is only ∼1.2-fold lower than those assigned for the bio-oil feed. Therefore, changes in the total number of detected/assigned molecular formulas, before and after hydrotreatment, do not provide insights into the effectiveness of the applied upgrading process. However, Figure 2b provides information about hypothetical recalcitrant oxygen-containing molecules (common formulas), whose characterization is critical to improving bio-oil upgrading methods. Among all of the effluents, RCFP-2 and RCFP-4 revealed the lowest numbers of common compositions to the bio-oil feed. It is essential to highlight that although common species have identical elemental composition, it is impossible to conclude that they are precisely the same entities before and after hydrotreatment, as they could be isomers. Furthermore, a fraction of common compositions might be generated by HDO. The compositional range of common species will be revisited later.

Figure 2c, the upper row, presents the combined DBE vs carbon number plots for all oxygen-containing molecules (*e.g.*, O_1, O_2, and O_3, O_4). The results indicate that the bio-oil feed featured a typical composition of wood-derived pyrolysis oils, with carbon numbers between 10 and 70 and DBE values from ∼1 to 35.[79] Individual plots for separate classes are included in the Supporting Information (Figure S1) and demonstrate that the bio-oil feed revealed trends in DBE and carbon number consistent with previous reports. Specifically, the data shows that DBE values and carbon numbers increased concurrently as a function of increasing oxygen number.[102,103] In general, at low oxygen numbers (*i.e.*, O_2−O_5), the addition of one oxygen atom increased the abundance-weighted-average (AW) DBE

https://doi.org/10.1021/acs.energyfuels.3c02599
Energy Fuels XXXX, XXX, XXX−XXX

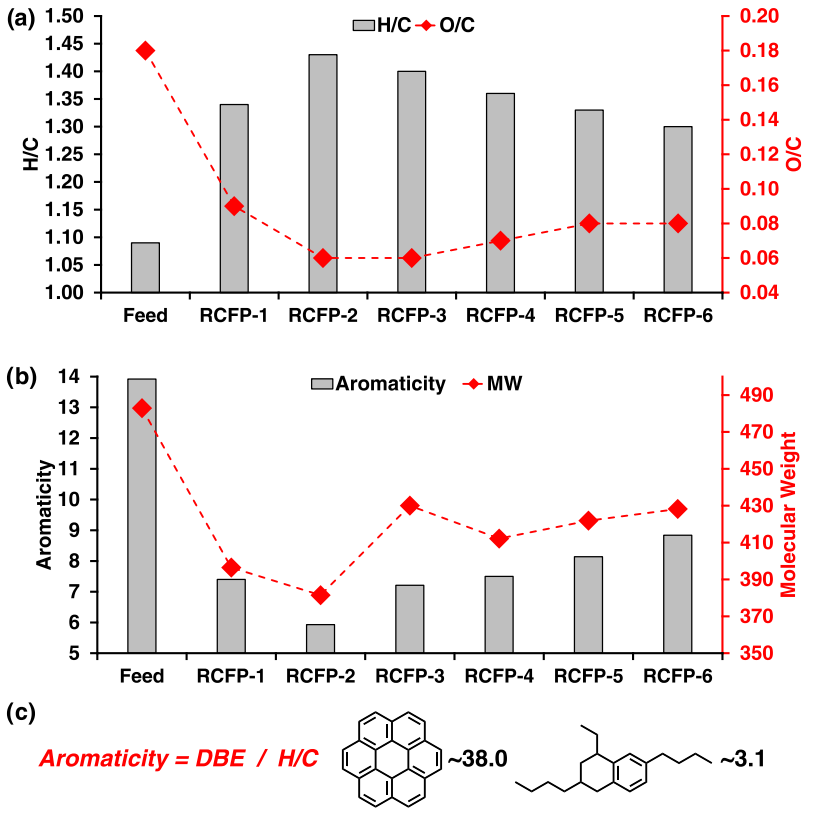

Figure 3. Abundance-weighted-average (AW) molecular features determined via −ESI coupled to 21 T FT-ICR MS: (a) H/C (gray bars) and O/C (red mark) ratios, (b) aromaticity (gray bars) and molecular weight (red mark), and (c) definition of aromaticity with examples of molecular structures.

by ∼1 unit and the AW carbon number by ∼2−2.5 units (Table S1 of the Supporting Information). This suggests the likely addition of furanic moieties to existing aromatic rings as highlighted in the Supporting Information (Figure S2).[104] At higher oxygen numbers (O_6−O_{11}), average changes in DBE and carbon numbers are less pronounced. For instance, the addition of two oxygen atoms (e.g., from O_8 to O_{10}) increased the AW DBE by ∼1 unit, adding ∼2−3 carbon atoms, which suggests the presence of heterocycles with multiple oxygen atoms (Figure S2).[104] Progression to even higher oxygen numbers (O_{12-13}) revealed minor changes in DBE and carbon number, which indicates the incorporation of O-containing functionalities such as OH. Collectively, these compositional trends point to the existence of sugarlike oligomers that survived the initial pyrolysis process to produce bio-oil.

The applied hydrotreatment produced significant changes in the composition, as shown in Figure 2c. Specifically, the global abundance-weighted DBE for the O-containing species for the bio-oil feed was 17.4; the values for all samples are included in the Supporting Information (Table S2). In contrast, the hydrotreated effluents revealed values between ∼10.4 and ∼13.4. Notably, the effluent RCFP-2 featured the lowest AW DBE (∼10.4) and carbon number (∼30). A recent work on hydrotreatment of lignin model compounds demonstrated that hydrodeoxygenation, apart from removing oxygen while increasing hydrogen, can promote cracking reactions that result in the loss of DBE.[105] It is essential to highlight that DBE values steadily increased from RCFP-3 (∼11.8) to RCFP-6 (∼13.4), which suggests a loss of hydrotreatment performance as a function of the increasing processing time.

Van Krevelen diagrams of atomic ratios such as H/C vs O/C can help understand the energy density of molecules (hydrogen content) and the oxygen content per carbon unit, two parameters critical for bio-oil applications.[81] Desired molecules for biorefinery have high H/C and low O/C and belong to zone 1, which is between $1.5 \leq H/C < 2$ and $0 < O/C \leq 0.3$. Conversely, unwanted molecules feature $0.5 < H/C < 1.5$ and $0 < O/C < 0.67$ (zone 2), and thus, their composition is more consistent with biochar.[106] Molecules with $1.5 < H/C < 2$, $O/C > 0.3$ are highly similar to lignin and belong to zone 3.[107] Zone 3 species can be "easily" transformed into compounds of zone 1.[81]

Figure 2c, the lower row, presents the van Krevelen diagrams for the bio-oil feed and the hydrotreated effluents and highlights zones 1, 2, and 3 for the feed, emphasizing zone 1 (red box) for the hydrotreated samples. The results indicate that the bio-oil feed featured a much wider compositional range than the effluents, with oxygen content between $\sim 0.05 < O/C < 0.60$ and H/C ratios from 0.5 to 2.0. The visual inspection of the van Krevelen diagrams suggests abundant content of highly aromatic, "low-quality" molecules of zone 2 for the feed, with low H/C and a wide range of O/C. Furthermore, the results show that the applied hydrotreatment effectively removed oxygen, as it produced abundant molecules with O/C ratios below 0.15. Importantly, a high proportion of bio-oil species "migrated" to zone 1 upon hydrotreatment, which was most pronounced for RCFP-1 and RCFP-2.

High-resolution mass spectrometry (HRMS) data analysis by molecular formula "counting" and average molecular parameters may expose trends that help elucidate optimal processing conditions and reaction pathways as demonstrated

https://doi.org/10.1021/acs.energyfuels.3c02599
Energy Fuels XXXX, XXX, XXX−XXX

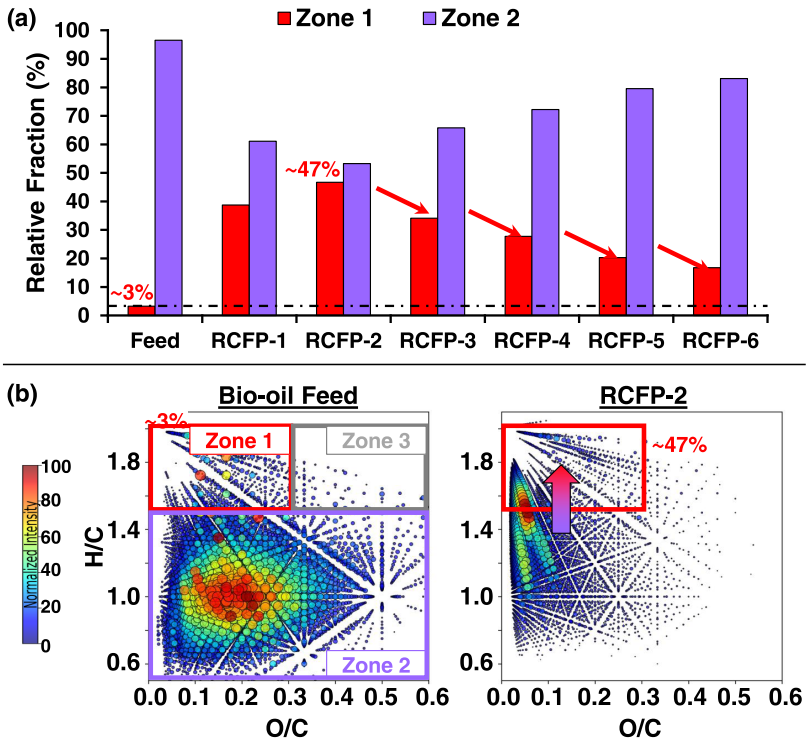

Figure 4. (a) Relative fraction of compositions present in each of the van Krevelen diagram zones previously defined by Palacio Lozano et al.[81] The data are derived from −ESI 21 T FT-ICR MS. (b) Expanded van Krevelen diagrams for O_X compounds for the bio-oil feed and the hydrotreated effluent RCFP-2.

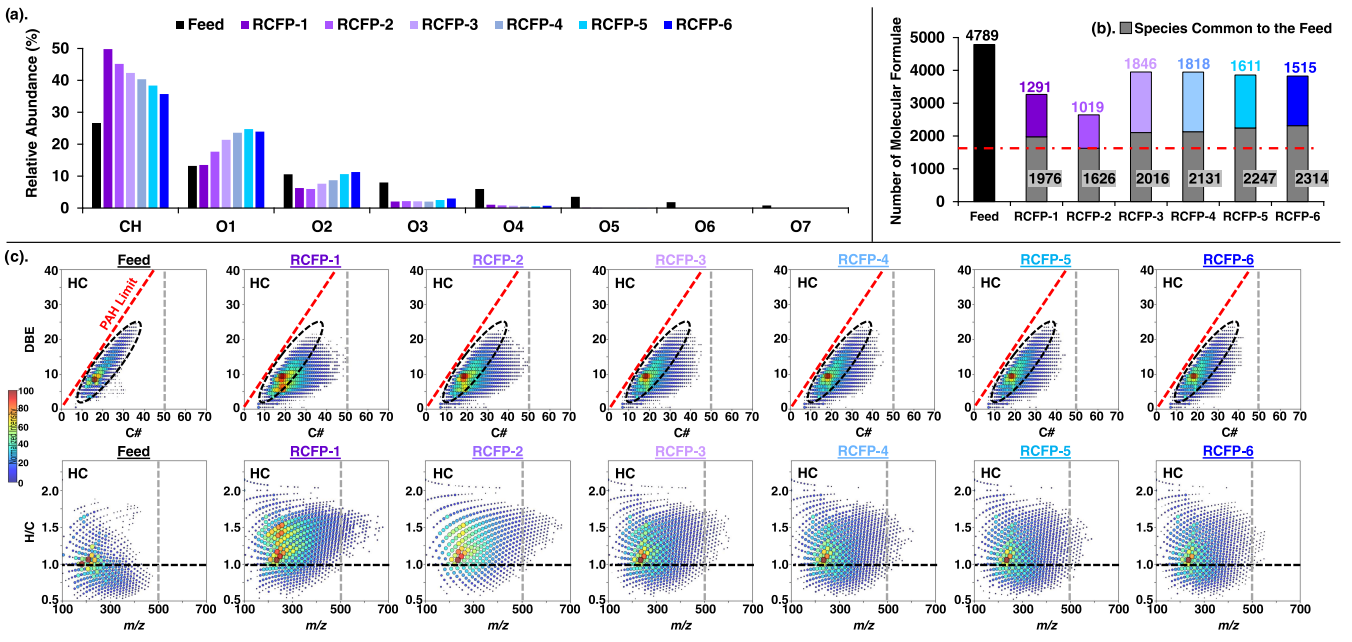

Figure 5. Molecular composition of the bio-oil feed and the hydrotreated effluents was determined by nC_7-assisted +APCI 12 T FT-ICR MS. (a) Compound class distribution, (b) number of common and unique molecular formulas relative to the bio-oil feed, and (c) compositional plots of DBE vs carbon numbers and H/C vs m/z for hydrocarbons or HC class.

for other complex mixtures.[81,108,109] Thus, Figure 3 presents FT-ICR MS-derived abundance-weighted H/C, O/C, molecular weight, and aromaticity. This work defines aromaticity as the ratio between the abundance-weighted DBE and the abundance-weighted H/C. Thus, molecules with high values of DBE but low H/C due to a limited content of CH_2 units, such as coronene (structure to the left in Figure 3c), have high aromaticity (~38.0). Conversely, compounds with low DBE but high alkyl substitution, such as the structure to the right in Figure 3c, present low aromaticity (~3.1). Figure 3 effectively summarizes the results from molecular characterization via FT-ICR MS. It clearly shows that the applied hydroprocessing successfully transformed the bio-oil feed into species with properties more consistent with those of conventional fuels.

https://doi.org/10.1021/acs.energyfuels.3c02599
Energy Fuels XXXX, XXX, XXX−XXX

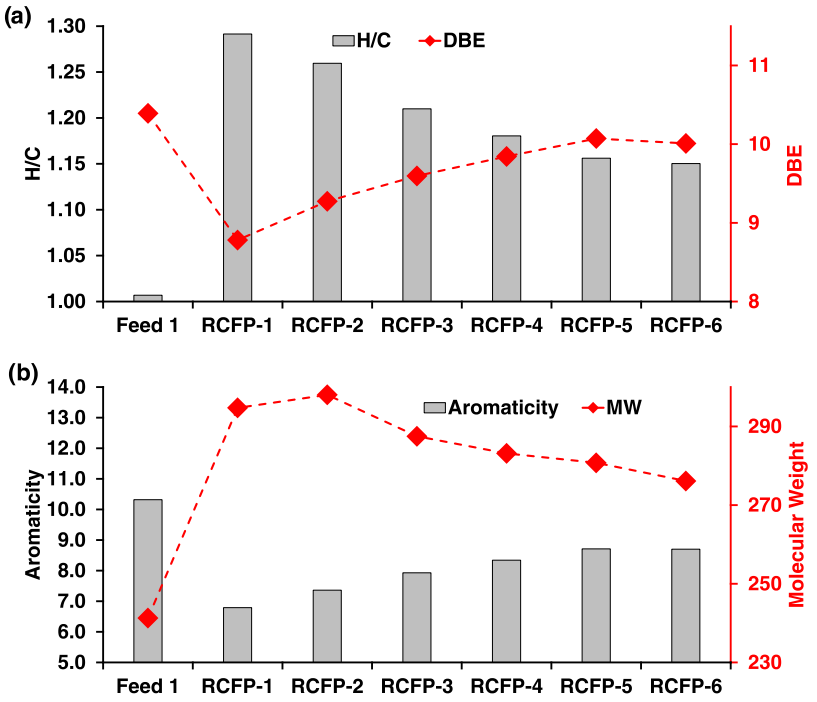

Figure 6. Abundance-weighted-average (AW) molecular features for the HC class derived from +APCI 12 T FT-ICR MS analysis of the bio-oil feed and the hydrotreated effluents. (a) H/C and DBE and (b) aromaticity and molecular weight. O/C ratios are not included as the data analysis is focused on the HC class.

Specifically, the bio-oil feed featured AW H/C < 1.10, O/C ∼ 0.18, average molecular weight (MW) of ∼480 g/mol, and aromaticity of ∼14. All of the hydrotreated effluents revealed increased H/C and pronounced decrease in O/C, MW, and aromaticity. The composition of the effluent RCFP-2 was particularly promising, with H/C > 1.4, a 3-fold decrease in O/C, less than half aromaticity, and ∼100 g/mol lower molecular weight than the bio-oil feed. The data shown in Figure 3 demonstrate that hydrotreatment performance significantly decreased after ∼48 h time on stream. Although all hydrotreated effluents revealed lower O content and aromaticity and higher H/C, catalyst deactivation was evident starting with RCFP-3 (collected at ∼72 h).

Relative Fraction of Molecules in "Bio-Oil Zones" of van Krevelen Diagrams. Figure 4a presents the relative fraction (RF) of compositions in zones 1, 2, and 3 of the van Krevelen diagrams for the bio-oil feed and the hydrotreated samples. RF was determined by eq 1, which divides the summed relative abundance for all assigned molecular formulas (RAi) for each separate zone, by the summed relative abundance of all compositions (total RA). The results indicate that all of the samples are depleted in zone 3 lignin-like species (<0.1%). Notably, the feed revealed ∼97% of highly aromatic compounds in zone 2 and only ∼3% of species in zone 1. Conversely, the effluent RCFP-2 featured the highest relative content of molecules in zone 1, ∼ 47%, which is ∼16-fold higher than that of the feed. The dramatic shift in composition is highlighted in the van Krevelen diagrams in Figure 4b. Notably, after ∼48 h time on stream, the amount of compounds in zone 1 dropped, which again points to a lower hydrotreatment performance likely due to catalyst deactivation. Several works have suggested that products from the polymerization of oxygen-containing species derived from biomass pyrolysis can cause fouling, which triggers catalyst deactivation and decreases deoxygenation and hydrogenation rates.[110−112]

$$\mathrm{RF} = \frac{\sum_{i=1}^{n} \mathrm{RAi}}{\text{Total RA}} \quad (1)$$

Access to Hydrocarbon Chemistry by Atmospheric Pressure Chemical Ionization Assisted with *n*-Heptane. nC_7-Assisted APCI is central to bio-oil characterization as it enables access to hydrocarbon species,[82] whose production is desired in biorefinery processes. Figure 5 presents the molecular composition of the bio-oil feed and hydrotreated effluents determined via +APCI 12 T FT-ICR MS. Figure 5a shows the compound class distribution and highlights the favored detection of hydrocarbons with no heteroatoms (HC class). It is critical to consider that APCI FT-ICR MS provided no direct quantification of hydrocarbons, opposite to GC × GC;[71,113] however, it revealed compositional trends that suggest a maximum content of hydrocarbons for RCFP-1−2. These effluents showed a ∼2-fold increase in relative abundance as compared with bio-oil feed. After ∼48 h of catalyst use (RCFP-2), the relative abundance of the HC class steadily decreased, with a concurrent increase in oxygen-containing classes, i.e., O_1 and O_2. As discussed earlier, elemental analysis confirmed the presence of N, whose bulk concentration raised upon hydrotreatment. It should be noted that a distinctive feature of pinewood is the elevated N content compared with fast-growing agricultural biomass.[114] It is likely that such species were not detected in −ESI, given their limited concentrations and much lower ionization efficiencies than those of the O_X classes.

Figure 5b shows that +APCI exposed trends consistent with −ESI: again, RCFP-2 featured the lowest number of molecular formulas common to the feed, and the number of common compositions increased continuously as a function of catalyst

https://doi.org/10.1021/acs.energyfuels.3c02599
Energy Fuels XXXX, XXX, XXX−XXX

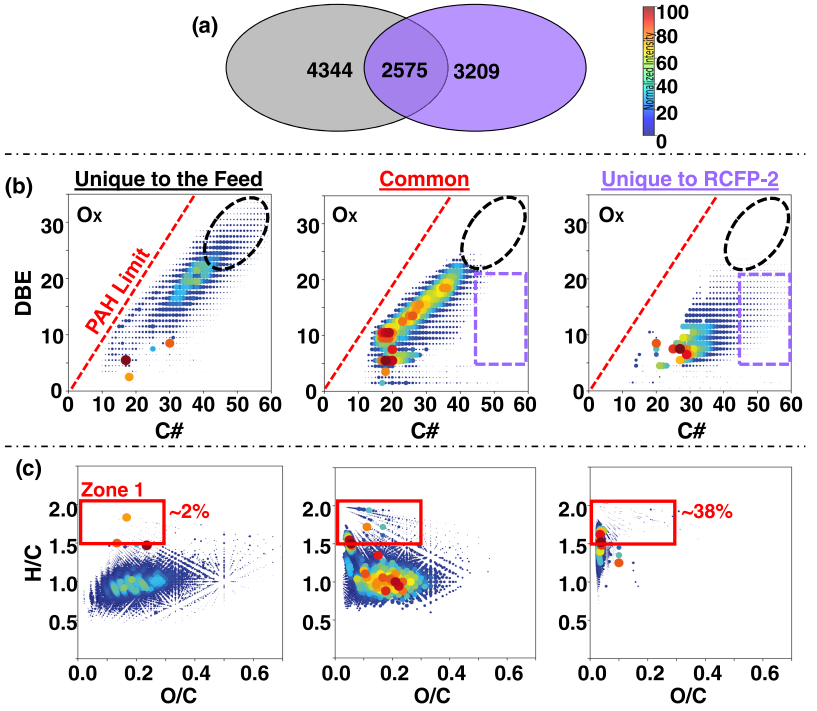

Figure 7. Number (a) and compositional range (b, c) for common and unique Ox molecular formulas to the bio-oil feed and RCFP-2. Data were derived from negative-ion ESI 21 T FT-ICR MS.

aging. We hypothesize that targeted analysis of common species is central to understanding the chemistry of recalcitrant compounds. Regarding the composition of hydrocarbons, Figure 5c presents their compositional range or DBE vs carbon number plots. The bio-oil feed revealed abundant alkyl-depleted HC species, which featured short homologous series or a limited range of carbon numbers for each DBE value.[115] As highlighted by the black-dashed circle, abundant compositions were detected adjacent to the PAH limit, which indicates a high content of alkyl-depleted polycyclic aromatic hydrocarbons. This finding is consistent with the well-known high production of PAHs from pyrolysis of lignin-enriched feedstocks.[116−118] Conversely, RCFP-2 featured a more extended homologous series, with carbon numbers up to ~50. Notably, the degree of alkyl substitution or homologous series length decreased as a function of increasing catalyst aging. For instance, RCFP-6 revealed compounds with carbon numbers of only up to ~40. Furthermore, the compositional plots of H/C vs m/z emphasize the abundant content of hydrocarbons with higher H/C ratios and molecular weights for the hydrotreated samples RCFP-1−2.

Again, the visual analysis of DBE vs carbon number plots and van Krevelen diagrams is challenging; therefore, Figure 6 summarizes the molecular properties of HC compounds as accessed by +APCI. The results indicate that RCFP-1−2 featured, among all hydrotreated effluents, the highest AW H/C and molecular weight and the lowest AW DBE and aromaticity. Comparison of Figures 3 and 6 shows that the feed revealed O_X compounds with higher aromaticity (~14, Figure 3b) than that of the HC species (~10, Figure 6b). Conversely, the hydrotreated samples comprised molecules with similar aromaticity, from ~6 to ~9, regardless of their oxygen content. This shows that the applied upgrading method was much more effective in increasing the hydrogen content of O_X species, as the applied HDO process targeted concurrent hydrogenation, transmethylation, and deoxygenation reactions for molecules with active O-containing moieties. Notably, the higher aromaticity of O-containing compounds in the feed indicates the abundant content of lignin-like residual structures.

Interestingly, changes in the average molecular weight were opposite for the O_X and HC classes. Hydrocarbons in RCFP-2 revealed an increase in ~60 g/mol compared to the feed, which could result from transalkylation reactions and the increase in H content. In contrast, the molecular weight of the O_X compounds decreased by ~100 g/mol after hydrotreatment. Interestingly, O_X species in RCFP-2 featured higher carbon numbers for low-DBE homologous series (Figure 2c). A potential increase in molecular weight due to the higher content of alkyl moieties could be offset by the cracking of lignin-like oligomers in the feed, which featured higher DBE values and carbon numbers. Additionally, global deoxygenation could contribute to the decrease in the molecular weight for the O_X species. Specifically, the abundance-weighted oxygen number decreased from ~5.6 (feed) to ~1.6 (RCFP-2). These compositional trends could explain why HC and the OC classes had opposite changes in the molecular weight. However, the DBE vs carbon number plots for O-containing compounds (Figure 2c) and HC class (Figure 5c) suggest that transalkylation reactions are not the only possible pathway to produce hydrocarbons with increased molecular weight than those present in the feed. In Figure 5, HC species in hydrotreated effluents reveal the same DBE range as in the feed but with a much more extended carbon number range, which indicates a higher content of CH_2 units. The carbon number range for HC species detected by +APCI is within the carbon number range of the Ox classes detected by −ESI (Figure 2c). Therefore, it is also possible that the increase in around 60 g/mol for HC in RCFP-2 is related to the production of hydrocarbons by deoxygenation of high-

https://doi.org/10.1021/acs.energyfuels.3c02599
Energy Fuels XXXX, XXX, XXX−XXX

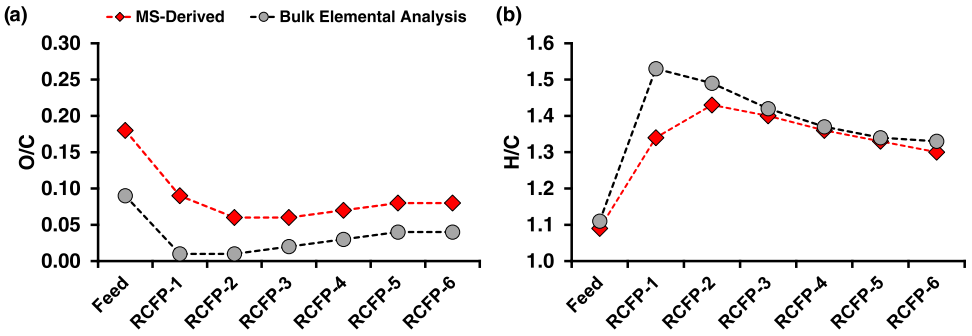

Figure 8. Graphic comparison for O/C (a) and H/C (b) ratios derived from bulk elemental analysis and −ESI 21 T FT-ICR MS.

molecular-weight O-containing species originally present in the feed.

Compositional Range for Common Molecular Formulas Detected in the Feed and RCFP-2. Figure 7a highlights the number of unique and common O_X formulas for the feed and the hydrotreated effluent RCFP-2. The compositional plots of DBE vs carbon numbers and van Krevelen diagrams are shown in panels (b) and (c). The data indicate that both samples have ∼2600 common compositions. Most common species revealed DBE values between ∼5 and 25, with high proximity to the PAH limit and dominant oxygen numbers between 2 and 5 (data shown in Figure 2a). This suggests that "recalcitrant" oxygen-containing molecules are, to some extent, highly aromatic and alkyl-depleted. Importantly, in this study, the O content was not completely removed. The highest O removal occurred from ∼8.3 to ∼1.0%. In this case, common species could be referred to as "intermediates" of the deoxygenation process, as they need further treatment, e.g., tandem HDO,[119] in order to achieve complete oxygen removal.

There is one group of unique molecules to the feed, circled in black, with DBE values > 20, extensive alkyl substitution (up to ∼25 carbon atoms in CH_2 units), and higher oxygen numbers (O_8−O_{13}, Figures 2a and S1). The absence of such compounds in RCFP-2 suggests the occurrence of cracking and hydrodeoxygenation of polymeric species with high oxygen numbers, which decreased the average molecular weight, DBE, and the O/C ratio. Indeed, species unique to RCFP-2 (especially the ones highlighted in purple in Figure 7b) belong to low-DBE (<20) homologous series with a higher content of alkyl moieties (higher carbon numbers). It is noteworthy an increase in carbon numbers has been observed after hydrodeoxygenation of model compounds. For instance, hydrodeoxygenation of anisole in the presence of Mo-based catalysts has shown the occurrence of transalkylation reactions to produce molecules with higher carbon numbers.[120] Furthermore, van Krevelen diagrams in Figure 7c indicate that a large fraction of unique species to RCFP-2 occupied the "optimal" bio-oil zone 1. Indeed, the relative fraction of unique molecules in zone 1 for RCFP-2 was ∼38% compared to only 2% for the feed. This suggests that the used hydrotreatment method can produce abundant new compositions with molecular features highly consistent with transportation fuels. In contrast, common molecular formulas between the biocrude feed and RCFP-2 mostly belong to zone 2 (96.7%), and only 3.2% of species correspond to zone 1.

Selective Ionization and Future Work. Complex mixture analysis by FT-ICR MS can be strikingly limited by selective ionization.[121,122] Importantly, ionization efficiency (ion production efficiency or "monomeric" ion yield) was consistent across the whole sample set. Ion production efficiency is inversely proportional to the accumulation period required to hit a target ion number (1×10^6 charges). On average, the bio-oil feed and effluents revealed accumulation periods (inject times) between 1.5 and 2.5 ms (∼2-fold difference average). Previous reports on petroleum analysis investigated samples with remarkably different ionization efficiencies. In those cases, accumulation periods in APPI varied between 40 and 2800 ms (∼70-fold difference).[123] However, there are still limitations on selective ionization evident from bulk elemental analysis. Figure 8 compares atomic ratios derived from bulk elemental analysis and −ESI 21 T FT-ICR MS. Clearly, −ESI favored the ionization of oxygen-enriched species, which likely suppressed the ionization of nonpolar compositions (HC), and thus, MS analysis yielded higher O/C values than those determined quantitatively. Furthermore, the effluents RCFP-1−2 revealed lower H/C ratios via MS than those determined by combustion elemental analysis. This indicates the preferred ionization of highly aromatic, alkyl-depleted compounds, known for their increased ionization efficiency in ESI compared to hydrogen-enriched molecules and overall inability of (−) ESI to capture the identity and diversity of HC products. Despite the discrepancies, both bulk elemental analysis and FT-ICR MS show similar trends allowing to conclude that ultra-high-resolution mass spectrometry is a convenient tool to understand bio-oil molecular composition, which is central in molecular management in biorefinery applications. Thus, our current efforts focus on understanding bio-oil chemistry by applying the lessons learned over two decades of research in petroleomics at the National High Magnetic Field Laboratory and other leading groups. Specifically, our goal is to develop separation methods for the nonvolatile fractions from bio-oils to overcome limitations from selective ionization and thus maximize the compositional range coverage and understanding of recalcitrant species and HC products. Previous efforts with fossil fuels demonstrate that separations can shorten the gap between atomic ratios derived from bulk elemental analysis and FT-ICR MS.[58] It is important to point out existing strategies based on chromatography,[124,125] extrography,[126] and derivatization reactions,[127] followed by solid-phase extraction,[128] whose further development is in course to investigate the samples discussed in this study.

CONCLUSIONS

High-field Fourier transform ion cyclotron resonance mass spectrometry was used to investigate the molecular composition of a Loblolly pine bio-oil and its hydrotreated effluents. As

https://doi.org/10.1021/acs.energyfuels.3c02599
Energy Fuels XXXX, XXX, XXX−XXX

in the early days of petroleomics, whole samples were analyzed with no previous chromatographic separations. Atomic ratios derived from FT-ICR MS revealed trends that resemble those from combustion elemental analysis. However, FT-ICR MS provided higher O/C and lower H/C ratios than bulk elemental analysis, which pointed to the preferential ionization of highly aromatic, oxygen-rich compositions. Despite such limitations, FT-ICR MS revealed a great potential to trace bio-oil molecular composition as a function of hydrotreatment time on stream and to comprehend the chemistry of recalcitrant, difficult-to-process species. Furthermore, the results highlighted the need to use different ion sources, i.e., ESI and APCI, to gain insight into different compound families, i.e., highly polar oxygen-rich species and hydrocarbons. In summary, FT-ICR MS showed that hydrotreating transformed the bio-oil feed or biocrude into fuel-range products when the HDO catalyst activity was high, but as the catalyst deactivated, the percentage of fuel-range molecules decreased. Regardless of the HDO catalyst activity, the high carbon number components identified in the biocrude feed seemed to be partially converted to lower carbon number products.

Data representation in van Krevelen diagrams exposed time-dependent compositional changes for the hydrotreated effluents and clearly highlighted the occurrence of catalyst deactivation. However, data visualization via van Krevelen diagrams can be a challenge to follow. Instead, compositional features derived from FT-ICR MS, such as abundance-weighted H/C, O/C, molecular weight, and aromaticity, were calculated and assisted in data interpretation. The results indicate that value-added hydrotreated effluents revealed hydrocarbons (HC class) in higher abundances compared with products obtained after catalyst deactivation. Such value-added bio-oils featured decreased oxygen content, aromaticity, and global molecular weight and revealed a marked increase in H/C. Specific molecular changes, concurrently visualized in DBE vs carbon number plots and van Krevelen diagrams, suggested distinct hydrotreatment reaction pathways, including concurrent deoxygenation and hydrogenation and cracking of highly aromatic lignin-like oligomers. Data analysis focused on common molecular formulas between the biocrude feed and the hydrotreated effluents indicates that recalcitrant or intermediate O-containing compounds are highly aromatic (low H/C) and alkyl-deficient.

One of the most significant lessons of decades of research in petroleomics is that separations are crucial to finding compositional trends that remain unseen when whole petroleum samples are analyzed. Therefore, current efforts are focused on the development of chromatographic methods to expand the compositional coverage through FT-ICR MS and target the separation of molecules from different zones of van Krevelen diagrams, i.e., high H/C and low O/C vs low H/C, which are the species close to the PAH limit in the DBE versus carbon number plots. However, the experience gained with fossil fuels indicates one big caveat: the higher the content of heteroatoms and polyfunctional molecules, the more challenging it is to develop optimal separation methods to target specific compound families. This will be the topic of our future reports.

■ ASSOCIATED CONTENT

Supporting Information

The Supporting Information is available free of charge at https://pubs.acs.org/doi/10.1021/acs.energyfuels.3c02599.

DBE vs carbon number plots for individual compound classes accessed via −ESI 21 T FT-ICR MS (Figure S1); molecular structure of softwood lignin and correlation with DBE and carbon number changes observed via −ESI 21 T FT-ICR MS for the bio-oil feed (Figure S2); abundance-weighted (AW) DBE, carbon number, and H/C for individual compound classes, derived from −ESI FT-ICR MS, for the feed bio-oil (Table S1); abundance-weighted (AW) DBE, carbon number, and H/C for all of the species detected via −ESI FT-ICR MS, for the feed bio-oil and the hydrotreated effluents (Table S2); and DBE vs carbon number plots for individual compound classes (e.g., O_1, O_2, O_3, etc.) accessed via +APCI 14-T FT-ICR MS (Figure S3) (PDF)

■ AUTHOR INFORMATION

Corresponding Author

Ryan P. Rodgers − *National High Magnetic Field Laboratory, Tallahassee, Florida 32310, United States; International Joint Laboratory for Complex Matrices Molecular Characterization, iC2MC, TRTG, 76700 Harfleur, France;* orcid.org/0000-0003-1302-2850; Email: rodgers@magnet.fsu.edu

Authors

Martha L. Chacón-Patiño − *National High Magnetic Field Laboratory, Tallahassee, Florida 32310, United States; International Joint Laboratory for Complex Matrices Molecular Characterization, iC2MC, TRTG, 76700 Harfleur, France;* orcid.org/0000-0002-7273-5343

Charlotte Mase − *International Joint Laboratory for Complex Matrices Molecular Characterization, iC2MC, TRTG, 76700 Harfleur, France; Normandie Université, COBRA, UMR 6014, FR 3038, Université de Rouen, INSA de Rouen, CNRS, IRCOF, Mont Saint Aignan Cedex 76821, France; TotalEnergies Refining & Chemicals, Total Research & Technology Gonfreville, 76700 Harfleur, France*

Julien Florent Maillard − *International Joint Laboratory for Complex Matrices Molecular Characterization, iC2MC, TRTG, 76700 Harfleur, France; TotalEnergies Refining & Chemicals, Total Research & Technology Gonfreville, 76700 Harfleur, France*

Caroline Barrère-Mangote − *International Joint Laboratory for Complex Matrices Molecular Characterization, iC2MC, TRTG, 76700 Harfleur, France; TotalEnergies Refining & Chemicals, Total Research & Technology Gonfreville, 76700 Harfleur, France*

David C. Dayton − *Technology Advancement and Commercialization, RTI International, Research Triangle Park, North Carolina 27709, United States;* orcid.org/0000-0003-3244-3722

Carlos Afonso − *International Joint Laboratory for Complex Matrices Molecular Characterization, iC2MC, TRTG, 76700 Harfleur, France; Normandie Université, COBRA, UMR 6014, FR 3038, Université de Rouen, INSA de Rouen, CNRS, IRCOF, Mont Saint Aignan Cedex 76821, France;* orcid.org/0000-0002-2406-5664

https://doi.org/10.1021/acs.energyfuels.3c02599
Energy Fuels XXXX, XXX, XXX−XXX

Pierre Giusti − *International Joint Laboratory for Complex Matrices Molecular Characterization, iC2MC, TRTG, 76700 Harfleur, France; Normandie Université, COBRA, UMR 6014, FR 3038, Université de Rouen, INSA de Rouen, CNRS, IRCOF, Mont Saint Aignan Cedex 76821, France; TotalEnergies Refining & Chemicals, Total Research & Technology Gonfreville, 76700 Harfleur, France*

Complete contact information is available at: https://pubs.acs.org/10.1021/acs.energyfuels.3c02599

Notes

The authors declare no competing financial interest.

■ ACKNOWLEDGMENTS

The authors thank RTI International for providing the samples and TotalEnergies for financial support through iC2MC. A portion of this work was performed in the Ion Cyclotron Resonance user facility at the National High Magnetic Field Laboratory in Tallahassee, Florida, which is supported by the National Science Foundation Division of Materials Research and Division of Chemistry through DMR-1644779 and the State of Florida. This work was also partially supported by University of Rouen Normandy, the European Regional Development Fund (ERDF, HN0001343), Labex SynOrg (Grant ANR-11- LABX-0029), Carnot Institute I2C, the Graduate School for Research XL-Chem (Grant ANR-18EURE-0020), the European Union's Horizon 2020 Research Infrastructures program (Grant Agreement 731077), and région Normandie. Access to the CNRS research infrastructure Infranalytics (FR2054) is gratefully acknowledged.

■ REFERENCES

(1) Sharma, M.; Singh, J.; Baskar, C.; Kumar, A. A Comprehensive Review of Renewable Energy Production from Biomass-Derived Bio-Oil. *Biotechnologia* **2019**, *100* (2), 179−194.

(2) Evans, R. J.; Milne, T. A. An American Chemical Society Journal. *Anal. Chem.* **1986**, *58* (13), 1370A.

(3) Carpenter, D.; Westover, T. L.; Czernik, S.; Jablonski, W. Biomass Feedstocks for Renewable Fuel Production: A Review of the Impacts of Feedstock and Pretreatment on the Yield and Product Distribution of Fast Pyrolysis Bio-Oils and Vapors. *Green Chem.* **2014**, *16* (2), 384−406.

(4) Dayton, D. C.; Mante, O. D.; Weiner, J.; Komnaris, C.; Verdier, S.; Gabrielsen, J. Integrated Reactive Catalytic Fast Pyrolysis: Biocrude Production, Upgrading, and Coprocessing. *Energy Fuels* **2022**, *36* (16), 9147−9157.

(5) Czernik, S.; Bridgwater, A. V. Overview of Applications of Biomass Fast Pyrolysis Oil. *Energy Fuels* **2004**, *18* (2), 590−598.

(6) Kuttiyathil, M. S.; Sivaramakrishnan, K.; Ali, L.; Shittu, T.; Z Iqbal, M.; Khaleel, A.; Altarawneh, M. Catalytic Upgrading of Pyrolytic Bio-Oil from Salicornia Bigelovii Seeds for Use as Jet Fuels: Exploring the Ex-Situ Deoxygenation Capabilities of Ni/Ze Catalyst. *Bioresour. Technol. Rep.* **2023**, *22* (February), No. 101437.

(7) Zheng, Y.; Wang, J.; Wang, D.; Zheng, Z. Advanced Catalytic Upgrading of Biomass Pyrolysis Vapor to Bio-Aromatics Hydrocarbon: A Review. *Appl. Energy Combust. Sci.* **2022**, *10* (March), No. 100061.

(8) Iyodo Mohammed, H.; Garba, K.; Isa Ahmed, S.; Garba Abubakar, L. Recent Advances on Strategies for Upgrading Biomass Pyrolysis Vapour to Value-Added Bio-Oils for Bioenergy and Chemicals. *Sustainable Energy Technol. Assess.* **2023**, *55* (December 2022), No. 102984.

(9) Kariim, I.; Waidi, Y. O.; Swai, H.; Kivevele, T. Catalytic Hydrothermal Liquefaction of Orange Peels into Biocrude: An Optimization Approach by Central Composite Design. *J. Anal. Appl. Pyrolysis* **2023**, *173* (June), No. 106032.

(10) Kilgore, U.; Santosa, D. M.; Li, S.; Wang, P.; Lee, S. J.; Thorson, M. R.; Ramasamy, K. Desalting Biocrude for Improved Downstream Processing toward Marine Fuel Application. *Sustainable Energy Fuels* **2023**, *7* (11), 2670−2679.

(11) Zacher, A. H.; Olarte, M. V.; Santosa, D. M.; Elliott, D. C.; Jones, S. B. A Review and Perspective of Recent Bio-Oil Hydrotreating Research. *Green Chem.* **2014**, *16* (2), 491−515.

(12) Environ, E.; Mettler, M. S.; Vlachos, G.; Dauenhauer, P. J. Top Ten Fundamental Challenges of Biomass Pyrolysis for Biofuels. *Energy Environ. Sci* **2012**, *5* (7), 7797−7809, DOI: 10.1039/c2ee21679e.

(13) Osman, A. I.; Farghali, M.; Ihara, I.; Elgarahy, A. M.; Ayyad, A.; Mehta, N.; Ng, K. H.; Abd El-Monaem, E. M.; Eltaweil, A. S.; Hosny, M.; Hamed, S. M.; Fawzy, S.; Yap, P. S.; Rooney, D. W. *Materials, Fuels, Upgrading, Economy, and Life Cycle Assessment of the Pyrolysis of Algal and Lignocellulosic Biomass: A Review*; Springer International Publishing, 2023; Vol. *21*. DOI: 10.1007/s10311-023-01573-7.

(14) Christensen, E.; Evans, R. J.; Carpenter, D. High-Resolution Mass Spectrometric Analysis of Biomass Pyrolysis Vapors. *J. Anal. Appl. Pyrolysis* **2017**, *124*, 327−334.

(15) Jarvis, M. W.; Olstad, J.; Parent, Y.; Deutch, S.; Iisa, K.; Christensen, E.; Ben, H.; Black, S.; Nimlos, M.; Magrini, K. Catalytic Upgrading of Biomass Pyrolysis Oxygenates with Vacuum Gas Oil Using a Davison Circulating Riser Reactor. *Energy Fuels* **2018**, *32* (2), 1733−1743.

(16) Seiser, R.; Olstad, J. L.; Magrini, K. A.; Jackson, R. D.; Peterson, B. H.; Christensen, E. D.; Talmadge, M. S. Co-Processing Catalytic Fast Pyrolysis Oil in an FCC Reactor. *Biomass Bioenergy* **2022**, *163* (April), No. 106484.

(17) Osman, A. I.; Abdelkader, A.; Farrell, C.; Rooney, D.; Morgan, K. Reusing, Recycling and up-Cycling of Biomass: A Review of Practical and Kinetic Modelling Approaches. *Fuel Process. Technol.* **2019**, *192* (January), 179−202.

(18) Osman, A. I. Mass Spectrometry Study of Lignocellulosic Biomass Combustion and Pyrolysis with NOx Removal. *Renewable Energy* **2020**, *146*, 484−496.

(19) Czernik, S.; Evans, R.; French, R. Hydrogen from Biomass-Production by Steam Reforming of Biomass Pyrolysis Oil. *Catal. Today* **2007**, *129* (3), 265−268.

(20) Oasmaa, A.; Czernik, S. Fuel Oil Quality of Biomass Pyrolysis Oils - State of the Art for the End Users. *Energy Fuels* **1999**, *13* (4), 914−921.

(21) Yang, H.; Yao, J.; Chen, G.; Ma, W.; Yan, B.; Qi, Y. Overview of Upgrading of Pyrolysis Oil of Biomass. *Energy Procedia* **2014**, *61*, 1306−1309.

(22) Resasco, D. E. What Should We Demand from the Catalysts Responsible for Upgrading Biomass Pyrolysis Oil? *J. Phys. Chem. Lett.* **2011**, *2* (18), 2294−2295.

(23) Ren, S.; Lei, H.; Wang, L.; Bu, Q.; Chen, S.; Wu, J. Hydrocarbon and Hydrogen-Rich Syngas Production by Biomass Catalytic Pyrolysis and Bio-Oil Upgrading over Biochar Catalysts. *RSC Adv.* **2014**, *4* (21), 10731−10737.

(24) Wang, W.; Liu, Y.; Liu, Z.; Tian, S. Detailed Chemical Composition of Straight-Run Vacuum Gas Oil and Its Distillates as a Function of the Atmospheric Equivalent Boiling Point. *Energy Fuels* **2016**, *30* (2), 968−974.

(25) Ben, H.; Wu, F.; Wu, Z.; Han, G.; Jiang, W.; Ragauskas, A. J. A Comprehensive Characterization of Pyrolysis Oil from Softwood Barks. *Polymers* **2019**, *11* (9), 1387.

(26) Elliott, D. C.; Hart, T. R.; Neuenschwander, G. G.; Rotness, L. J.; Olarte, M. V.; Zacher, A. H.; Solantausta, Y. Catalytic Hydroprocessing of Fast Pyrolysis Bio-Oil from Pine Sawdust. *Energy Fuels* **2012**, *26* (6), 3891−3896.

(27) Talmadge, M. S.; Baldwin, R. M.; Biddy, M. J.; McCormick, R. L.; Beckham, G. T.; Ferguson, G. A.; Czernik, S.; Magrini-Bair, K. A.; Foust, T. D.; Metelski, P. D.; Hetrick, C.; Nimlos, M. R. A Perspective

on Oxygenated Species in the Refinery Integration of Pyrolysis Oil. *Green Chem.* **2014**, *16* (2), 407−453.
(28) Dayton, D. C.; Mante, O. D.; Weiner, J. Effect of Temperature on the Pilot-Scale Catalytic Pyrolysis of Loblolly Pine. *Energy Fuels* **2021**, *35* (16), 13181−13190.
(29) Ren, X.; Meng, J.; Chang, J.; Kelley, S. S.; Jameel, H.; Park, S. Effect Of Blending Ratio Of Loblolly Pine Wood And Bark On The Properties Of Pyrolysis Bio-Oils. *Fuel Process. Technol.* **2017**, *167*, 43−49.
(30) Pan, S.; Pu, Y.; Foston, M.; Ragauskas, A. J. Compositional Characterization and Pyrolysis of Loblolly Pine and Douglas-Fir Bark. *Bioenergy Res.* **2013**, *6* (1), 24−34.
(31) Meng, J.; Moore, A.; Tilotta, D.; Kelley, S.; Park, S. Toward Understanding of Bio-Oil Aging: Accelerated Aging of Bio-Oil Fractions. *ACS Sustainable Chem. Eng.* **2014**, *2* (8), 2011−2018.
(32) Huang, F.; Singh, P. M.; Ragauskas, A. J. Characterization of Milled Wood Lignin (MWL) in Loblolly Pine Stem Wood, Residue, and Bark. *J. Agric. Food Chem.* **2011**, *59* (24), 12910−12916.
(33) Chen, Q. M.; Hu, Z.; Chang, H. M.; Li, B. Micro Analytical Methods for Determination of Compression Wood Content in Loblolly Pine. *J. Wood Chem. Technol.* **2007**, *27* (3−4), 169−178.
(34) Yeh, T. F.; Chang, H. M.; Kadla, J. F. Rapid Prediction of Solid Wood Lignin Content Using Transmittance Near-Infrared Spectroscopy. *J. Agric. Food Chem.* **2004**, *52* (6), 1435−1439.
(35) Yeh, T.-F.; Braun, J. L.; Goldfarb; Barry, C.; Hang, H.; Kadla, J. F. *Chemical and Structural Characterizations of Juvenile Wood, Mature Wood, and Compression Wood of Loblolly Pine (Pinus Taeda), 2005*; North Carolina State University, 2006. DOI: 10.1515/HF.2006.001.
(36) Acquah, G. E.; Via, B. K.; Gallagher, T.; Billor, N.; Fasina, O. O.; Eckhardt, L. G. High Throughput Screening of Elite Loblolly Pine Families for Chemical and Bioenergy Traits with near Infrared Spectroscopy. *Forests* **2018**, *9* (7), 418.
(37) Wang, K.; Dayton, D. C.; Peters, J. E.; Mante, O. D. Reactive Catalytic Fast Pyrolysis of Biomass to Produce High-Quality Bio-Crude. *Green Chem.* **2017**, *19* (14), 3243−3251.
(38) Cross, P.; Wang, K.; Weiner, J.; Reid, E.; Peters, J.; Mante, O.; Dayton, D. C. Reactive Catalytic Fast Pyrolysis of Biomass over Molybdenum Oxide Catalysts: A Parametric Study. *Energy Fuels* **2020**, *34* (4), 4678−4684.
(39) Eschenbacher, A.; Saraeian, A.; Shanks, B. H.; Jensen, P. A.; Li, C.; Duus, J. Ø.; Hansen, A. B.; Mentzel, U. V.; Henriksen, U. B.; Ahrenfeldt, J.; Jensen, A. D. Enhancing Bio-Oil Quality and Energy Recovery by Atmospheric Hydrodeoxygenation of Wheat Straw Pyrolysis Vapors Using Pt and Mo-Based Catalysts. *Sustainable Energy Fuels* **2020**, *4* (4), 1991−2008.
(40) Nolte, M. W.; Shanks, B. H. A Perspective on Catalytic Strategies for Deoxygenation in Biomass Pyrolysis. *Energy Technol.* **2017**, *5* (1), 7−18.
(41) Hemberger, P.; Custodis, V. B. F.; Bodi, A.; Gerber, T.; Van Bokhoven, J. A. Understanding the Mechanism of Catalytic Fast Pyrolysis by Unveiling Reactive Intermediates in Heterogeneous Catalysis. *Nat. Commun.* **2017**, *8* (May), No. 15946.
(42) Lyu, G.; Wu, S.; Zhang, H. Estimation and Comparison of Bio-Oil Components from Different Pyrolysis Conditions. *Front. Energy Res.* **2015**, *3* (JUN), 28.
(43) Balat, M. An Overview of the Properties and Applications of Biomass Pyrolysis Oils. *Energy Sources, Part A Recover. Util. Environ. Eff.* **2011**, *33* (7), 674−689.
(44) Jones, S.; Valkenburg, C.; Walton, C.; Elliott, D.; Holladay, J.; Stevens, D.; Kinchin, C.; Czernik, S. *Production of Gasoline and Diesel from Biomass via Fast Pyrolysis, Hydrotreating and Hydrocracking: A Design Case*, Office of Scientific and Technical Information, 2009, No. February, 76. PNNL-22684.pdf.
(45) Shemfe, M. B.; Gu, S.; Ranganathan, P. Techno-Economic Performance Analysis of Biofuel Production and Miniature Electric Power Generation from Biomass Fast Pyrolysis and Bio-Oil Upgrading. *Fuel* **2015**, *143*, 361−372.
(46) Oasmaa, A.; Elliott, D. C.; Prins, W. Virtual Special Issue of Recent Advances in Biofuel Production via Co-Refining Route. *Energy Fuels* **2023**, *37* (10), 6875−6878.
(47) Parrilla-Lahoz, S.; Jin, W.; Pastor-Pérez, L.; Duyar, M. S.; Martínez-Quintana, L.; Dongil, A. B.; Reina, T. R. Multicomponent Graphene Based Catalysts for Guaiacol Upgrading in Hydrothermal Conditions: Exploring "H2-Free" Alternatives for Bio-Compounds Hydrodeoxygenation. *Catal. Today* **2023**, *423* (November 2022), 114020 DOI: 10.1016/j.cattod.2023.01.027.
(48) Dimitriadis, A.; Bergvall, N.; Johansson, A. C.; Sandström, L.; Bezergianni, S.; Tourlakidis, N.; Meca, L.; Kukula, P.; Raymakers, L. Biomass Conversion via Ablative Fast Pyrolysis and Hydroprocessing towards Refinery Integration: Industrially Relevant Scale Validation. *Fuel* **2023**, *332* (2), No. 126153.
(49) Saidi, M.; Moradi, P. Sustainable Biofuel Production via Catalytic Hydrodeoxygenation of 4-Methylanisole over Mo/Nano γ-Al2O3. *Chem. Eng. Process. - Process Intensif.* **2023**, *191* (June), No. 109447.
(50) Christensen, E. D.; Chupka, G. M.; Luecke, J.; Smurthwaite, T.; Alleman, T. L.; Iisa, K.; Franz, J. A.; Elliott, D. C.; McCormick, R. L. Analysis of Oxygenated Compounds in Hydrotreated Biomass Fast Pyrolysis Oil Distillate Fractions. *Energy Fuels* **2011**, *25* (11), 5462−5471.
(51) Freeman, C. J.; Jones, S. B.; Padmaperuma, A. B.; Santosa, D. M.; Valkenburg, C.; Shinn, J.*Initial Assessment of U.S. Refineries for Purposes of Potential Bio-Based Oil Insertions*; Office of Scientific and Technical Information, 2013. DOI: 10.2172/1097335.
(52) Patil, M. L.; Lali, A. M.; Dalai, A. K. Catalytic Hydrodeoxygenation of Bio-Oil Model Compound for Production of Fuel Grade Oil. *Asia-Pac. J. Chem. Eng.* **2019**, *14* (4), No. e2317.
(53) Lee, H.; Kim, H.; Yu, M. J.; Ko, C. H.; Jeon, J. K.; Jae, J.; Park, S. H.; Jung, S. C.; Park, Y. K. Catalytic Hydrodeoxygenation of Bio-Oil Model Compounds over Pt/HY Catalyst. *Sci. Rep.* **2016**, *6*, No. 28765.
(54) Nolte, M. W.; Zhang, J.; Shanks, B. H. Ex Situ Hydrodeoxygenation in Biomass Pyrolysis Using Molybdenum Oxide and Low Pressure Hydrogen. *Green Chem.* **2016**, *18* (1), 134−138.
(55) Murugappan, K.; Mukarakate, C.; Budhi, S.; Shetty, M.; Nimlos, M. R.; Román-Leshkov, Y. Supported Molybdenum Oxides as Effective Catalysts for the Catalytic Fast Pyrolysis of Lignocellulosic Biomass. *Green Chem.* **2016**, *18* (20), 5548−5557.
(56) Church, A. L.; Hu, M. Z.; Lee, S. J.; Wang, H.; Liu, J. Selective Adsorption Removal of Carbonyl Molecular Foulants from Real Fast Pyrolysis Bio-Oils. *Biomass Bioenergy* **2020**, *136* (July 2019), No. 105522.
(57) Palacio-Lozano, D. C.; Thomas, M. J.; Jones, H. E.; Barrow, M. P. Petroleomics: Tools, Challenges, and Developments. *Annu. Rev. Anal. Chem.* **2020**, *13*, 405−430.
(58) Chacón-Patiño, M. L.; Gray, M. R.; Rüger, C.; Smith, D. F.; Glattke, T. J.; Niles, S. F.; Neumann, A.; Weisbrod, C. R.; Yen, A.; McKenna, A. M.; Giusti, P.; Bouyssiere, B.; Barrère-Mangote, C.; Yarranton, H.; Hendrickson, C. L.; Marshall, A. G.; Rodgers, R. P. Lessons Learned from a Decade-Long Assessment of Asphaltenes by Ultrahigh-Resolution Mass Spectrometry and Implications for Complex Mixture Analysis. *Energy Fuels* **2021**, *35* (20), 16335−16376.
(59) Abdelnur, P. V.; Vaz, B. G.; Rocha, J. D.; De Almeida, M. B. B.; Teixeira, M. A. G.; Pereira, R. C. L. Characterization of Bio-Oils from Different Pyrolysis Process Steps and Biomass Using High-Resolution Mass Spectrometry. *Energy Fuels* **2013**, *27* (11), 6646−6654.
(60) Marshall, A. G.; Rodgers, R. P. Petroleomics: The Next Grand Challenge For Chemical Analysis. *Acc. Chem. Res.* **2004**, *37*, 53−59.
(61) Rodgers, R. P.; Mckenna, A. M.; Robbins, W. K.; Hsu, S.; Lu, J.; Hendrickson, C. L.; Christopher, M.; Nelson, R. K.; Marshall, A. G. Petroleomics: Past, Present and Future. 2011, *56* (2), 429−430.
(62) Mullins, O. C.Petroleomics and Structure−Function Relations of Crude Oils and Asphaltenes. In *Asphaltenes, Heavy Oils, and Petroleomics*; Springer: New York, 2007; pp 1−16. DOI: 10.1007/0-387-68903-6_1.

https://doi.org/10.1021/acs.energyfuels.3c02599
Energy Fuels XXXX, XXX, XXX−XXX

(63) Boduszynski, M. M. Composition of Heavy Petroleums. 1. Molecular Weight, Hydrogen Deficiency, and Heteroatom Concentration as a Function of Atmospheric Equivalent Boiling Point up to 1400 °F (760 °C). *Energy Fuels* **1987**, *1* (1), 2−11.
(64) Chacón-Patiño, M. L.; Rowland, S. M.; Rodgers, R. P. The Compositional and Structural Continuum of Petroleum from Light Distillates to Asphaltenes: The Boduszynski Continuum Theory As Revealedby FT-ICR Mass Spectrometry. In *The Boduszynski Continuum: Contributions to the Understanding of the Molecular Composition of Petroleum*; Ovalles, C.; Moir, M. E., Eds.; ACS Symposium Series; American Chemical Society: Washington, DC, 2018; Vol. *1282*, pp 113−171.
(65) Nyadong, L.; Lai, J.; Thompsen, C.; LaFrancois, C. J.; Cai, X.; Song, C.; Wang, J.; Wang, W. High-Field Orbitrap Mass Spectrometry and Tandem Mass Spectrometry for Molecular Characterization of Asphaltenes. *Energy Fuels* **2018**, *32* (1), 294−305.
(66) Gray, M. R.; Chacón-Patiño, M. L.; Rodgers, R. P. Structure−Reactivity Relationships for Petroleum Asphaltenes. *Energy Fuels* **2022**, *36*, 4370.
(67) Rodgers, R. P.; Marshall, A. G. Petroleomics: Advanced Characterization of Petroleum-Derived Materials by Fourier Transform Ion Cyclotron Resonance Mass Spectrometry (FT-ICR MS). In *Asphaltenes, Heavy Oils, and Petroleomics*; Mullins, O. C.; Sheu, E. Y.; Hammam, A.; Marshall, A. G., Eds.; Springer, 2007; pp 63−93.
(68) He, Z.; Wang, X. Hydrodeoxygenation of Model Compounds and Catalytic Systems for Pyrolysis Bio-Oils Upgrading. *Catal. Sustainable Energy* **2012**, *1*, 28−52.
(69) Staš, M.; Auersvald, M.; Vozka, P. Two-Dimensional Gas Chromatography Characterization of Pyrolysis Bio-Oils: A Review. *Energy Fuels* **2021**, *35* (10), 8541−8557.
(70) Undri, A.; Abou-Zaid, M.; Briens, C.; Berruti, F.; Rosi, L.; Bartoli, M.; Frediani, M.; Frediani, P. A Simple Procedure for Chromatographic Analysis of Bio-Oils from Pyrolysis. *J. Anal. Appl. Pyrolysis* **2015**, *114*, 208−221.
(71) Palacio Lozano, D. C.; Jones, H. E.; Gavard, R.; Thomas, M. J.; Ramírez, C. X.; Wootton, C. A.; Sarmiento Chaparro, J. A.; O'Connor, P. B.; Spencer, S. E. F.; Rossell, D.; Mejia-Ospino, E.; Witt, M.; Barrow, M. P. Revealing the Reactivity of Individual Chemical Entities in Complex Mixtures: The Chemistry behind Bio-Oil Upgrading. *Anal. Chem.* **2022**, *94* (21), 7536−7544.
(72) Tessarolo, N. S.; Silva, R. C.; Vanini, G.; Pinho, A.; Romão, W.; de Castro, E. V. R.; Azevedo, D. A. Assessing the Chemical Composition of Bio-Oils Using FT-ICR Mass Spectrometry and Comprehensive Two-Dimensional Gas Chromatography with Time-of-Flight Mass Spectrometry. *Microchem. J.* **2014**, *117*, 68−76.
(73) Hertzog, J.; Carré, V.; Le Brech, Y.; Dufour, A.; Aubriet, F. Toward Controlled Ionization Conditions for ESI-FT-ICR-MS Analysis of Bio-Oils from Lignocellulosic Material. *Energy Fuels* **2016**, *30* (7), 5729−5739.
(74) Marshall, A. G.; Rodgers, R. P. Petroleomics: Chemistry of the Underworld. *Proc. Natl. Acad. Sci. U.S.A.* **2008**, *105* (47), 18090−18095.
(75) Herzsprung, P.; Hertkorn, N.; Von Tümpling, W.; Harir, M.; Friese, K.; Schmitt-Kopplin, P. Molecular Formula Assignment for Dissolved Organic Matter (DOM) Using High-Field FT-ICR-MS: Chemical Perspective and Validation of Sulphur-Rich Organic Components (CHOS) in Pit Lake Samples. *Anal. Bioanal. Chem.* **2016**, *408* (10), 2461−2469.
(76) Palacio Lozano, D. C.; Thomas, M. J.; Jones, H. E.; Barrow, M. P. Petroleomics: Tools, Challenges, and Developments. *Annu. Rev. Anal. Chem.* **2020**, *13*, 405−430.
(77) Jarvis, J. M.; Page-Dumroese, D. S.; Anderson, N. M.; Corilo, Y.; Rodgers, R. P. Characterization of Fast Pyrolysis Products Generated from Several Western USA Woody Species. *Energy Fuels* **2014**, *28* (10), 6438−6446.
(78) Staš, M.; Chudoba, J.; Kubička, D.; Blažek, J.; Pospíšil, M. Petroleomic Characterization of Pyrolysis Bio-Oils: A Review. *Energy Fuels* **2017**, *31* (10), 10283−10299.
(79) Ware, R. L. L.; Rodgers, R. P.; Marshall, A. G.; Mante, O. D.; Dayton, D. C.; Verdier, S.; Gabrielsen, J.; Rowland, S. M. Detailed Chemical Composition of an Oak Biocrude and Its Hydrotreated Product Determined by Positive Atmospheric Pressure Photoionization Fourier Transform Ion Cyclotron Resonance Mass Spectrometry. *Sustainable Energy Fuels* **2020**, *4* (5), 2404−2410.
(80) Ware, R. L.; Rodgers, R. P.; Marshall, A. G.; Mante, O. D.; Dayton, D. C.; Verdier, S.; Gabrielsen, J.; Rowland, S. M. Tracking Elemental Composition through Hydrotreatment of an Upgraded Pyrolysis Oil Blended with a Light Gas Oil. *Energy Fuels* **2020**, *34* (12), 16181−16186.
(81) Palacio Lozano, D. C.; Jones, H. E.; Ramirez Reina, T.; Volpe, R.; Barrow, M. P. Unlocking the Potential of Biofuels: Via Reaction Pathways in van Krevelen Diagrams. *Green Chem.* **2021**, *23* (22), 8949−8963.
(82) Mase, C.; Hubert-Roux, M.; Afonso, C.; Giusti, P. Contribution of Atmospheric Pressure Chemical Ionization Mass Spectrometry for the Characterization of Bio-Oils from Lignocellulosic Biomass: Comparison with Electrospray Ionization and Atmospheric Pressure Photoionization. *J. Anal. Appl. Pyrolysis* **2022**, *167*, No. 105694.
(83) Manheim, J. M.; Milton, J. R.; Zhang, Y.; Kenttämaa, H. I. Fragmentation of Saturated Hydrocarbons upon Atmospheric Pressure Chemical Ionization Is Caused by Proton-Transfer Reactions. *Anal. Chem.* **2020**, *92* (13), 8883−8892.
(84) Tose, L. V.; Cardoso, F. M. R.; Fleming, F. P.; Vicente, M. A.; Silva, S. R. C.; Aquije, G. M. F. V.; Vaz, B. G.; Romão, W. Analyzes of Hydrocarbons by Atmosphere Pressure Chemical Ionization FT-ICR Mass Spectrometry Using Isooctane as Ionizing Reagent. *Fuel* **2015**, *153*, 346−354.
(85) Bahureksa, W.; Borch, T.; Young, R. B.; Weisbrod, C. R.; Blakney, G. T.; McKenna, A. M. Improved Dynamic Range, Resolving Power, and Sensitivity Achievable with FT-ICR Mass Spectrometry at 21 T Reveals the Hidden Complexity of Natural Organic Matter. *Anal. Chem.* **2022**, *94* (32), 11382−11389.
(86) Lobodin, V. V.; Juyal, P.; Mckenna, A. M.; Rodgers, R. P.; Marshall, A. G. Tetramethylammonium Hydroxide as a Reagent for Complex Mixture Analysis by Negative Ion Electrospray Ionization Mass Spectrometry. *Anal. Chem.* **2013**, *85*, 7803−7808.
(87) Hendrickson, C. L.; Quinn, J. P.; Kaiser, N. K.; Smith, D. F.; Blakney, G. T.; Chen, T.; Marshall, A. G.; Weisbrod, C. R.; Beu, S. C. 21 T Fourier Transform Ion Cyclotron Resonance Mass Spectrometer: A National Resource for Ultrahigh Resolution Mass Analysis. *J. Am. Soc. Mass Spectrom.* **2015**, *26* (9), 1626−1632.
(88) Smith, D. F.; Podgorski, D. C.; Rodgers, R. P.; Blakney, G. T.; Hendrickson, C. L. 21 Tesla FT-ICR Mass Spectrometer for Ultrahigh-Resolution Analysis of Complex Organic Mixtures. *Anal. Chem.* **2018**, *90* (3), 2041−2047.
(89) Chacón-Patiño, M. L.; Moulian, R.; Barrère-Mangote, C.; Putman, J. C.; Weisbrod, C. R.; Blakney, G. T.; Bouyssiere, B.; Rodgers, R. P.; Giusti, P. Compositional Trends for Total Vanadium Content and Vanadyl Porphyrins in Gel Permeation Chromatography Fractions Reveal Correlations between Asphaltene Aggregation and Ion Production Efficiency in Atmospheric Pressure Photoionization. *Energy Fuels* **2020**, *34* (12), 16158−16172.
(90) Savory, J. J.; Kaiser, N. K.; Mckenna, A. M.; Xian, F.; Blakney, G. T.; Rodgers, R. P.; Hendrickson, C. L.; Marshall, A. G. Parts-Per-Billion Fourier Transform Ion Cyclotron Resonance Mass Measurement Accuracy with a "Walking" Calibration Equation. *Anal. Chem.* **2011**, *83*, 1732−1736.
(91) Corilo, Y. E. PetroOrg Software; Florida State University; All rights reserved, 2013 http://www.petroorg.com.
(92) Sueur, M.; Maillard, J. F.; Lacroix-andrivet, O.; Rüger, C. P.; et al. PyC2MC: An Open-Source Software Solution for Visualization and Treatment of High-Resolution Mass Spectrometry Data. *J. Am. Soc. Mass Spectrom.* **2023**, *34* (4), 617−626, DOI: 10.1021/jasms.2c00323.
(93) Marshall, A. G.; Rodgers, R. P. Petroleomics: The Next Grand Challenge for Chemical Analysis. *Acc. Chem. Res.* **2004**, *37* (1), 53−59.

https://doi.org/10.1021/acs.energyfuels.3c02599
Energy Fuels XXXX, XXX, XXX−XXX

(94) Rowland, S. M.; Robbins, W. K.; Corilo, Y. E.; Marshall, A. G.; Rodgers, R. P. Solid-Phase Extraction Fractionation To Extend the Characterization of Naphthenic Acids in Crude Oil by Electrospray Ionization Fourier Transform Ion Cyclotron Resonance Mass Spectrometry. *Energy Fuels* **2014**, *28*, 5043−5048.
(95) Clingenpeel, A. C.; Rowland, S. M.; Corilo, Y. E.; Zito, P.; Rodgers, R. P. Fractionation of Interfacial Material Reveals a Continuum of Acidic Species That Contribute to Stable Emulsion Formation. *Energy Fuels* **2017**, *31* (6), 5933−5939.
(96) Rodgers, R. P.; Mapolelo, M. M.; Robbins, W. K.; Chacón-Patiño, M. L.; Putman, J. C.; Niles, S. F.; Rowland, S. M.; Marshall, A. G. Combating Selective Ionization in the High Resolution Mass Spectral Characterization of Complex Mixtures. *Faraday Discuss.* **2019**, *218*, 29.
(97) Peru, K. M.; Thomas, M. J.; Palacio Lozano, D. C.; McMartin, D. W.; Headley, J. V.; Barrow, M. P. Characterization of Oil Sands Naphthenic Acids by Negative-Ion Electrospray Ionization Mass Spectrometry: Influence of Acidic versus Basic Transfer Solvent. *Chemosphere* **2019**, *222* (1), 1017−1024.
(98) Cho, Y.; Kim, Y. H.; Kim, S. Planar Limit-Assisted Structural Interpretation of Saturates/Aromatics/Resins/Asphaltenes Fractionated Crude Oil Compounds Observed by Fourier Transform Ion Cyclotron Resonance Mass Spectrometry. *Anal. Chem.* **2011**, *83* (15), 6068−6073.
(99) Lobodin, V. V.; Marshall, A. G.; Hsu, C. S. Compositional Space Boundaries for Organic Compounds. *Anal. Chem.* **2012**, *84*, 3410−3416.
(100) Chacón-Patiño, M. L.; Blanco-Tirado, C.; Orrego-Ruiz, J. A.; Gómez-Escudero, A.; Combariza, M. Y. Tracing the Compositional Changes of Asphaltenes after Hydroconversion and Thermal Cracking Processes by High-Resolution Mass Spectrometry. *Energy Fuels* **2015**, *29* (10), 6330−6341.
(101) Glattke, T. J.; Chacón-Patiño, M. L.; Hoque, S. S.; Ennis, T. E.; Greason, S.; Marshall, A. G.; Rodgers, R. P. Complex Mixture Analysis of Emerging Contaminants Generated from Coal Tar- and Petroleum-Derived Pavement Sealants: Molecular Compositions and Correlations with Toxicity Revealed by Fourier Transform Ion Cyclotron Resonance Mass Spectrometry. *Environ. Sci. Technol.* **2022**, *56* (18), 12988−12998.
(102) Jarvis, J. M.; McKenna, A. M.; Hilten, R. N.; Das, K. C.; Rodgers, R. P.; Marshall, A. G. Characterization of Pine Pellet and Peanut Hull Pyrolysis Bio-Oils by Negative-Ion Electrospray Ionization Fourier Transform Ion Cyclotron Resonance Mass Spectrometry. *Energy Fuels* **2012**, *26* (6), 3810−3815.
(103) Catalina, D.; Lozano, P.; Ramírez, C. X.; Sarmiento, J. A.; Thomas, M. J.; Gavard, R.; Jones, H. E.; Cabanzo, R. Characterization of Bio-Crude Components Derived from Pyrolysis of Soft Wood and Its Esterified Product by Ultrahigh Resolution Mass Spectrometry and Spectroscopic Techniques. *Fuel* **2020**, *259*, No. 116085.
(104) Lu, X.; Gu, X. A Review on Lignin Pyrolysis: Pyrolytic Behavior, Mechanism, and Relevant Upgrading for Improving Process Efficiency. *Biotechnol. Biofuels. Bioprod.* **2022**, *15* (1), No. 106, DOI: 10.1186/s13068-022-02203-0.
(105) Jiang, W.; Cao, J.; Xie, J.; Zhao, L.; Zhang, C.; Zhao, X.; Zhao, Y.; Zhang, J. Catalytic Hydrodeoxygenation of Lignin and Its Model Compounds to Hydrocarbon Fuels over a Metal/Acid Ru/HZSM - 5 Catalyst. *Energy Fuels* **2021**, *35*, 19543−19552.
(106) McKenna, A. M.; Chacón-Patiño, M. L.; Chen, H.; Blakney, G. T.; Mentink-Vigier, F.; Young, R. B.; Ippolito, J. A.; Borch, T. Expanding the Analytical Window for Biochar Speciation: Molecular Comparison of Solvent Extraction and Water-Soluble Fractions of Biochar by FT-ICR Mass Spectrometry. *Anal. Chem.* **2021**, *93* (46), 15365−15372.
(107) Laszakovits, J. R.; MacKay, A. A. Data-Based Chemical Class Regions for Van Krevelen Diagrams. *J. Am. Soc. Mass Spectrom.* **2022**, *33* (1), 198−202.
(108) Chacón-Patiño, M. L.; Smith, D. F.; Hendrickson, C. L.; Marshall, A. G.; Rodgers, R. P. Advances in Asphaltene Petroleomics. Part 4. Compositional Trends of Solubility Subfractions Reveal That Polyfunctional Oxygen-Containing Compounds Drive Asphaltene Chemistry. *Energy Fuels* **2020**, *34*, 3013−3030.
(109) Rogel, E.; Moir, M.; Witt, M. Atmospheric Pressure Photoionization and Laser Desorption Ionization Coupled to Fourier Transform Ion Cyclotron Resonance Mass Spectrometry to Characterize Asphaltene Solubility Fractions: Studying the Link between Molecular Composition and Physical Behavior. *Energy Fuels* **2015**, *29* (7), 4201−4209.
(110) Weber, R. S.; Olarte, M. V.; Wang, H. Modeling the Kinetics of Deactivation of Catalysts during the Upgrading of Bio-Oil. *Energy Fuels* **2015**, *29* (1), 273−277.
(111) Qiao, Z.; Wang, Z.; Zhang, C.; Yuan, S.; Zhu, Y.; Wang, J.; Wang, S. PVAm−PIP/PS Composite Membrane with High Performance for CO_2/N_2 Separation. *AIChE J.* **2013**, *59* (4), 215−228.
(112) Olarte, M. V.; Zacher, A. H.; Padmaperuma, A. B.; Burton, S. D.; Job, H. M.; Lemmon, T. L.; Swita, M. S.; Rotness, L. J.; Neuenschwander, G. N.; Frye, J. G.; Elliott, D. C. Stabilization of Softwood-Derived Pyrolysis Oils for Continuous Bio-Oil Hydroprocessing. *Top. Catal.* **2016**, *59* (1), 55−64.
(113) Chiaramonti, D.; Buffi, M.; Rizzo, A. M.; Prussi, M.; Martelli, F. Bio-Hydrocarbons through Catalytic Pyrolysis of Used Cooking Oils: Towards Sustainable Jet and Road Fuels. *Energy Procedia* **2015**, *82*, 343−349.
(114) Negahdar, L.; Gonzalez-Quiroga, A.; Otyuskaya, D.; Toraman, H. E.; Liu, L.; Jastrzebski, J. T. B. H.; Van Geem, K. M.; Marin, G. B.; Thybaut, J. W.; Weckhuysen, B. M. Characterization and Comparison of Fast Pyrolysis Bio-Oils from Pinewood, Rapeseed Cake, and Wheat Straw Using 13C NMR and Comprehensive GC × GC. *ACS Sustainable Chem. Eng.* **2016**, *4* (9), 4974−4985.
(115) Schrader, W.; Panda, S. K.; Brockmann, K. J.; Benter, T. Characterization of Non-Polar Aromatic Hydrocarbons in Crude Oil Using Atmospheric Pressure Laser Ionization and Fourier Transform Ion Cyclotron Resonance Mass Spectrometry (APLI FT-ICR MS). *Analyst* **2008**, *133* (7), 867.
(116) Lee, H.; Jae, J.; Lee, H. W.; Park, S.; Jeong, J.; Lam, S. S.; Park, Y. K. Production of Bio-Oil with Reduced Polycyclic Aromatic Hydrocarbons via Continuous Pyrolysis of Biobutanol Process Derived Waste Lignin. *J. Hazard. Mater.* **2020**, *384* (July 2019), No. 121231.
(117) Fabbri, D.; Adamiano, A.; Torri, C. GC-MS Determination of Polycyclic Aromatic Hydrocarbons Evolved from Pyrolysis of Biomass. *Anal. Bioanal. Chem.* **2010**, *397* (1), 309−317.
(118) Kim, Y. M.; Lee, H. W.; Jang, S. H.; Jeong, J.; Ryu, S.; Jung, S. C.; Park, Y. K. Production of Biofuels from Pine Needle via Catalytic Fast Pyrolysis over HBeta. *Korean J. Chem. Eng.* **2020**, *37* (3), 493−496.
(119) Yeboah, I.; Li, Y.; Rajendran, K.; Rout, K. R.; Chen, D. Tandem Hydrodeoxygenation Catalyst System for Hydrocarbons Production from Simulated Bio-Oil : Effect of C−C Coupling Catalysts. *Ind. Eng. Chem. Res.* **2021**, *60* (5), 2136−2143, DOI: 10.1021/acs.iecr.1c00113.
(120) Wang, H.; Male, J.; Wang, Y. Recent Advances in Hydrotreating of Pyrolysis Bio-Oil and Its Oxygen-Containing Model Compounds. *ACS Catal.* **2013**, *3* (5), 1047−1070.
(121) Cho, Y.; Na, J.; Nho, N.; Kim, S.; Kim, S. Application of Saturates, Aromatics, Resins, and Asphaltenes Crude Oil Fractionation for Detailed Chemical Characterization of Heavy Crude Oils by Fourier Transform Ion Cyclotron Resonance Mass Spectrometry Equipped with Atmospheric Pressure Photoionization. *Energy Fuels* **2012**, *26*, 2558−2565.
(122) Chacón-Patiño, M. L.; Vesga-Martínez, S. J.; Blanco-Tirado, C.; Orrego-Ruiz, J. A.; Gómez-Escudero, A.; Combariza, M. Y. Exploring Occluded Compounds and Their Interactions with Asphaltene Networks Using High-Resolution Mass Spectrometry. *Energy Fuels* **2016**, *30* (6), 4550−4561.
(123) Chacón-Patiño, M. L.; Rowland, S. M.; Rodgers, R. P. Advances in Asphaltene Petroleomics. Part 2: Selective Separation Method That Reveals Fractions Enriched in Island and Archipelago

https://doi.org/10.1021/acs.energyfuels.3c02599
Energy Fuels XXXX, XXX, XXX−XXX

Structural Motifs by Mass Spectrometry. *Energy Fuels* **2018**, *32* (1), 314−328.
(124) Ware, R. L.; Rowland, S. M.; Lu, J.; Rodgers, R. P.; Marshall, A. G. Compositional and Structural Analysis of Silica Gel Fractions from Municipal Waste Pyrolysis Oils. *Energy Fuels* **2018**, *32* (7), 7752−7761.
(125) Rowland, S. M.; Smith, D. F.; Blakney, G. T.; Corilo, Y. E.; Hendrickson, C. L.; Rodgers, R. P. Online Coupling of Liquid Chromatography with Fourier Transform Ion Cyclotron Resonance Mass Spectrometry at 21 T Provides Fast and Unique Insight into Crude Oil Composition. *Anal. Chem.* **2021**, *93*, 13749−13754.
(126) Chacón-Patiño, M. L.; Rowland, S. M.; Rodgers, R. P. Advances in Asphaltene Petroleomics. Part 2: Selective Separation Method That Reveals Fractions Enriched in Island and Archipelago Structural Motifs by Mass Spectrometry. *Energy Fuels* **2018**, *32* (1), 314−328.
(127) Palacio Lozano, D. C.; Jones, H. E.; Barrow, M. P.; Wills, M. Chemoselective Derivatisation and Ultrahigh Resolution Mass Spectrometry for the Determination of Hydroxyl Functional Groups within Complex Bio-Oils. *RSC Adv.* **2023**, *13* (26), 17727−17741.
(128) Niles, S. F.; Chacón-Patiño, M. L.; Chen, H.; Mckenna, A. M.; Blakney, G. T.; Rodgers, R. P.; Marshall, A. G. Molecular-Level Characterization of Oil-Soluble Ketone/Aldehyde Photo-Oxidation Products by Fourier Transform Ion Cyclotron Resonance Mass Spectrometry Reveals Similarity Between Microcosm and Field Samples. *Environ. Sci. Technol.* **2019**, *53*, 6887−6894.

https://doi.org/10.1021/acs.energyfuels.3c02599
Energy Fuels XXXX, XXX, XXX−XXX